CCL2-induced chemokine cascade promotes breast cancer metastasis by enhancing retention of metastasis-associated macrophages

Takanori Kitamura,[1] Bin-Zhi Qian,[1] Daniel Soong,[1] Luca Cassetta,[1] Roy Noy,[2] Gaël Sugano,[1] Yu Kato,[2] Jiufeng Li,[2] and Jeffrey W. Pollard[1,2]

[1]MRC Centre for Reproductive Health, Queen's Medical Research Institute, the University of Edinburgh, Edinburgh EH16 4TJ, Scotland, UK
[2]Department of Developmental and Molecular Biology, Center for the Study of Reproductive Biology and Women's Health, Albert Einstein College of Medicine, New York, NY 10461

Pulmonary metastasis of breast cancer cells is promoted by a distinct population of macrophages, metastasis-associated macrophages (MAMs), which originate from inflammatory monocytes (IMs) recruited by the CC-chemokine ligand 2 (CCL2). We demonstrate here that, through activation of the CCL2 receptor CCR2, the recruited MAMs secrete another chemokine ligand CCL3. Genetic deletion of CCL3 or its receptor CCR1 in macrophages reduces the number of lung metastasis foci, as well as the number of MAMs accumulated in tumor-challenged lung in mice. Adoptive transfer of WT IMs increases the reduced number of lung metastasis foci in *Ccl3* deficient mice. Mechanistically, *Ccr1* deficiency prevents MAM retention in the lung by reducing MAM–cancer cell interactions. These findings collectively indicate that the CCL2-triggered chemokine cascade in macrophages promotes metastatic seeding of breast cancer cells thereby amplifying the pathology already extant in the system. These data suggest that inhibition of CCR1, the distal part of this signaling relay, may have a therapeutic impact in metastatic disease with lower toxicity than blocking upstream targets.

CORRESPONDENCE
Jeffrey W. Pollard:
Jeff.Pollard@ed.ac.uk

Abbreviations used: BMDM, BM-derived macrophage; BMT, BM transplantation; CCL, CC-chemokine ligand; CCR, CC-chemokine receptor; GEM, genetically engineered mouse; IM, inflammatory monocyte; MAM, metastasis-associated macrophage; MDM, monocyte-derived macrophage; PyMT, Polyoma Middle T oncogene; RM, resident monocyte.

Breast cancer is a leading cause of cancer death, largely because of metastatic disease (Jemal et al., 2011). There are a large numbers of clinical studies that indicate a strong correlation between poor prognosis of the disease and high infiltration of macrophages in the tumor (Bingle et al., 2002; Knowles and Harris, 2007). For example, high macrophage infiltration strongly associates with reduced relapse-free and overall survival of breast cancer patients (Leek, et al., 1996). The intensive infiltration of macrophages is also found in a genetically engineered mouse (GEM) model of breast cancer caused by the mammary epithelial restricted expression of the Polyoma Middle T oncogene (PyMT; Lin et al., 2001, 2003). Importantly, ablation of macrophages in the PyMT mice through a null mutation of colony-stimulating factor 1 gene (*Csf1*$^{op/op}$) dramatically suppressed lung metastases (Lin et al., 2001), which indicates pivotal roles of macrophages in breast cancer pulmonary metastasis.

It has been reported that macrophages are diverse and contain many different populations that play specific roles in developmental process, tissue repair, inflammatory responses, and tumor development (Pollard, 2009; Davies et al., 2013). In mice, macrophages are characterized by their high expression of surface markers such as F4/80 and CD68, and no expression of Ly6G. In the lung of the PyMT mice with metastatic lesions, there are at least two distinct macrophage populations: F4/80$^+$CD11c$^+$ and F4/80$^+$CD11b$^+$ macrophages (Qian et al., 2009). The F4/80$^+$CD11c$^+$ macrophages are alveolar macrophages that also exist in the normal lung. Although these CD11c$^+$ resident macrophages are required for clearance of cellular debris and initiation of inflammatory responses (Hussell

The Rockefeller University Press $30.00
J. Exp. Med. 2015 Vol. 212 No. 7 1043–1059
www.jem.org/cgi/doi/10.1084/jem.20141836

and Bell, 2014), they are not involved in breast cancer metastasis (Qian et al., 2009). In contrast, the CD11b$^+$ macrophages are recruited by metastasizing cancer cells but are few in number in normal lung. In an experimental metastasis model of breast cancer, these CD11b$^+$ macrophages are recruited and in direct contact with disseminating cancer cells within 48 h after tumor injection, which promotes extravasation of cancer cells. Because depletion of the CD11b$^+$ macrophages reduces the number and size of metastatic foci in the lung (Qian et al., 2009), the recruitment of these metastasis-associated macrophages (MAMs) is essential for extravasation and persistent growth of breast cancer cells.

We have recently reported that adoptively transferred inflammatory monocytes (IMs) characterized as CD11b$^+$Ly6C^{high} preferentially migrate to the lung with metastatic tumors than the primary tumor (Qian et al., 2011). We have also found that treatment with antibodies against the CC-chemokine ligand 2 (CCL2) suppresses the recruitment of IMs and reduces the number of MAMs in the lung, indicating that MAMs originate from circulating IMs. Because IMs express the CCL2 receptor CCR2 at high levels and anti-CCL2 antibody treatments reduce the number of metastatic foci, the CCL2–CCR2 axis plays an important role in metastatic seeding of breast cancer cells via recruitment of IMs. Our results thus suggest CCL2 as a potential therapeutic target to prevent the MAM-mediated tumor metastasis. However, anti-CCL2 antibody is ineffective at suppressing free CCL2 in humans (Sandu et al., 2013). Moreover, loss of CCL2 signaling severely depresses numbers of circulating monocytes that increases susceptibility to infection in mouse models (Serbina et al., 2008), suggesting the requirement for alternative targets to suppress prometastatic function of MAMs.

Although CCL2 is known as a monocyte chemoattractant (Matsushima et al., 1989), it also promotes phagocytosis, survival, and polarization of myeloid cells (Roca et al., 2009; Tanaka et al., 2010). We thus hypothesized that the CCL2–CCR2 axis may regulate functions of MAMs, and could be another mechanism underlying MAM-mediated metastatic seeding of cancer cells. Accordingly, we have found that the recruited MAMs also express CCR2 (Qian et al., 2009), and loss of *Ccr2* reduces ability of macrophages to support cancer cell extravasation in vitro (Qian et al., 2011). Here, we demonstrate a novel role of the CCL2–CCR2 axis in breast cancer metastasis. We show that activation of CCR2 signaling prompts MAMs to secrete another chemokine, CCL3. The increased CCL3 secretion results in enhanced MAM–cancer cell interaction and prolonged retention of MAMs in the metastasis sites, which promotes extravasation of cancer cells. These data identify a novel prometastatic chemokine cascade that promotes lung metastasis.

RESULTS

Activation of CCL2–CCR2 axis increases CCL3 secretion from MAMs

To test our hypothesis that CCR2 acts as a signaling receptor in MAMs, we first identified potential downstream targets of CCR2 signaling in the MAMs. Previously, we reported that CD11b$^+$ MAMs express a much higher level of CCR2 compared with CD11c$^+$ pulmonary resident macrophages (Qian et al., 2009), suggesting that MAMs receive more CCR2 signal than resident macrophages. We therefore compared the gene expression profile of MAMs (F4/80$^+$CD11b$^+$) with those of resident macrophages in normal lung (Lng MΦ; F4/80$^+$CD11c$^+$) and similarly isolated splenic (Spl MΦ; F4/80$^+$CD11b$^+$) macrophages. Hierarchical clustering clearly separated MAMs from other resident macrophages, and identified 37 genes whose expression was significantly higher in MAMs (Fig. 1, A and B). To narrow down the candidates, we compared mRNA levels of these genes between WT and *Ccr2*-deficient macrophages and found eight genes whose expression was significantly reduced in *Ccr2*-deficient macrophages (Fig. 1 C). Notably, one of these genes encodes the CC-chemokine ligand 3 (CCL3), a high-affinity ligand for CCR1 (Neote et al., 1993) whose expression in myeloid cells is associated with metastasis of colon cancer and lymphoma cells (Kitamura et al., 2010; Rodero et al., 2013). It is also reported that CCL3 enhances intracellular calcium flux in human macrophages but not monocytes (Kaufmann et al., 2001), suggesting that CCL3 might possess specific roles in macrophage functions. We thus hypothesized that activation of CCL2–CCR2 signaling prompts macrophages to secrete CCL3, which regulates prometastatic functions of MAMs.

Consistent with the results from the microarray and real-time PCR, we found 40–50% reduction in CCL3 protein secretion from *Ccr2*-deficient macrophages compared with that from WT macrophages (Fig. 2, A and B). In the WT macrophages, stimulation with recombinant CCL2 significantly increased CCL3 mRNA and protein expression (Fig. 2 B). Because such an increase in CCL3 secretion was not found in *Ccr2*-deficient macrophages (Fig. 2 B), these results indicate that CCL2 signaling via CCR2 can increase CCL3 secretion from macrophages. Recombinant CCL2 failed to increase CCL3 secretion in *Ccr2*$^{-/-}$ BMDMs, and thus it is unlikely that any increase in CCL3 secretion is induced by contaminating endotoxin. Indeed, endotoxin contamination is reported as <0.01 ng/ml in our culture conditions and this is much less than is needed to increase CCL3 secretion from alveolar and peritoneal macrophages (Wang et al., 2000). To investigate whether CCL2 promotes *Ccl3* expression in MAMs in vivo, we injected anti-CCL2 neutralizing antibody into WT mice having a similar load of lung metastases. After 2 d of antibody treatment, we isolated MAMs (F4/80$^+$CD11b$^+$CD11c$^-$Ly6C$^-$) and resident pulmonary macrophages (F4/80$^+$CD11b$^-$CD11c$^+$Ly6C$^-$) from tumor-bearing lung and inflammatory monocytes (IM; CD115$^+$CD11b$^+$Ly6C$^+$) and resident monocytes (RM; CD115$^+$CD11b$^+$Ly6C$^-$) from peripheral blood (Fig. S1). The treatment with anti-CCL2 antibody significantly suppressed *Ccl3* transcript levels in MAMs (Fig. 2 C), indicating that CCL2 can increase CCL3 expression in macrophages at the metastasis sites as well. Interestingly, MAMs expressed 10-fold higher *Ccl3* mRNA compared with either circulating IMs or RMs, or resident macrophages in the lung. It is notable that other major leukocyte populations in the

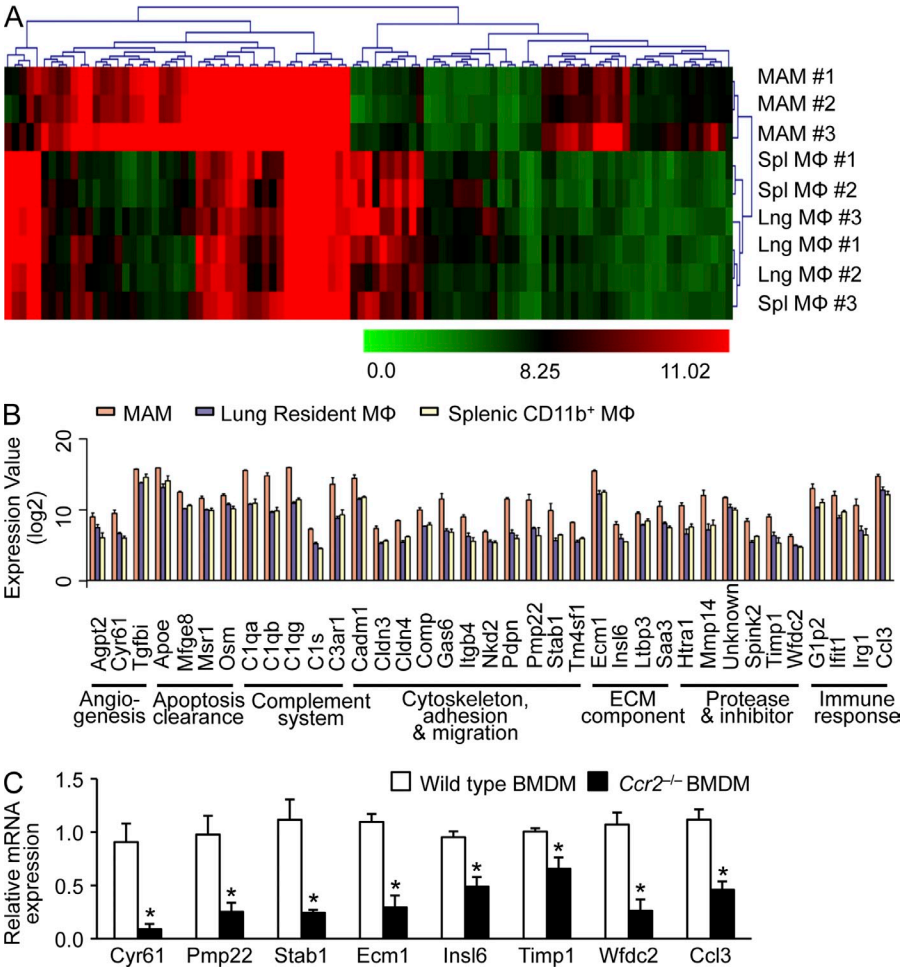

Figure 1. Identification of MAM-specific genes regulated by CCR2 signaling in mice. (A) Heat maps of unsupervised hierarchical clustering of microarray analysis of RNA isolated from MAMs (F4/80$^+$CD11b$^+$) compared with those from resident lung macrophages (Lng; F4/80$^+$CD11c$^+$) and splenic macrophages (Spl; F4/80$^+$CD11b$^+$). MAMs were isolated from mice injected with Met-1 mouse breast cancer cells (n = 3/group). Color bars show intensity of gene expression. (B) Genes differentially regulated in MAMs (more than threefold change; $P < 0.01$, ANOVA) were clustered according to GO terms. Data on expression values are presented as means ± SEM. Note that the scale is exponential. (A and B) data were derived from three independent repeats for each sample group. (C) The relative mRNA expression of candidate genes (as indicated) was assessed by RT-PCR in BMDMs isolated from WT or *Ccr2*$^{-/-}$ mice (n = 3, three independent experiments). Data are means ± SEM. *, $P < 0.05$.

tumor-bearing lung expressed low levels of *Ccl3* mRNA comparable with resident macrophages, suggesting MAMs are the major source of CCL3 in the metastasis site (Fig. 2 D). Consistent with these data, *CCL3* mRNA level in human monocyte-derived macrophages (hMDMs) was significantly higher than freshly isolated monocytes, and this level was increased by recombinant human CCL2 (Fig. 2, E and F). We have reported that CCL3 secretion from cultured macrophages is increased by conditioned medium from mouse mammary tumor cells (Ojalvo et al., 2009). Likewise, conditioned medium from various subtypes of human breast cancer cells increased *CCL3* levels in hMDMs (Fig. 2 G). The conditioned medium contained CCL2 (MDA435, 56.5 ± 3.7; MDA231, 37.8 ± 5.2; T47D, 13.0 ± 0.6; MCF7, 59.4 ± 3.5 pg/ml), and the increase in *CCL3* by the conditioned medium from MDA231 cells that induced highest amount of CCL3 was suppressed by anti-human CCL2 antibody treatment (67% compared with control IgG treatment; Fig. 2 H). The anti-CCL2 antibody treatment also suppressed *CCL3* expression induced by conditioned medium from MDA435 (78% compared with control IgG treatment) but not from T47D and MCF7 cells (unpublished data). Collectively, these results indicate that MAMs secrete high level of CCL3 once they differentiate from IMs, and it is regulated, at least in part, by the CCL2–CCR2 signaling pathway. Our results, however, do not exclude the contribution of other pathways in the regulation of CCL3 synthesis.

CCL3 secretion from MAMs promotes metastatic seeding of breast cancer cells

Although the role of CCL3 in breast cancer metastasis remains unclear, oncomine search results (Farmer et al., 2005; Finak et al., 2008) indicated that *CCL3* was up-regulated in breast cancer stroma and in basal-like invasive breast carcinoma that are predicted to have poor prognoses (Fig. 3 A). These results suggest that stromal expression of CCL3 is involved in breast cancer progression. To investigate the role of CCL3 in breast cancer metastasis, we injected MDA-MB-231:4175 cells expressing luciferase (Minn et al., 2005) into the mammary fat pad of nude mice as a model for human triple negative breast cancer. The recipient nude mice were irradiated and transplanted with BM cells from immunodeficient mice (*Rag2*$^{-/-}$) or those that are homozygous for the *Ccl3*-null allele (*Rag2*$^{-/-}$*Ccl3*$^{-/-}$) before tumor implantation so that we could investigate the role of CCL3 from BM cells. 4 wk after tumor injection, we resected the primary tumor

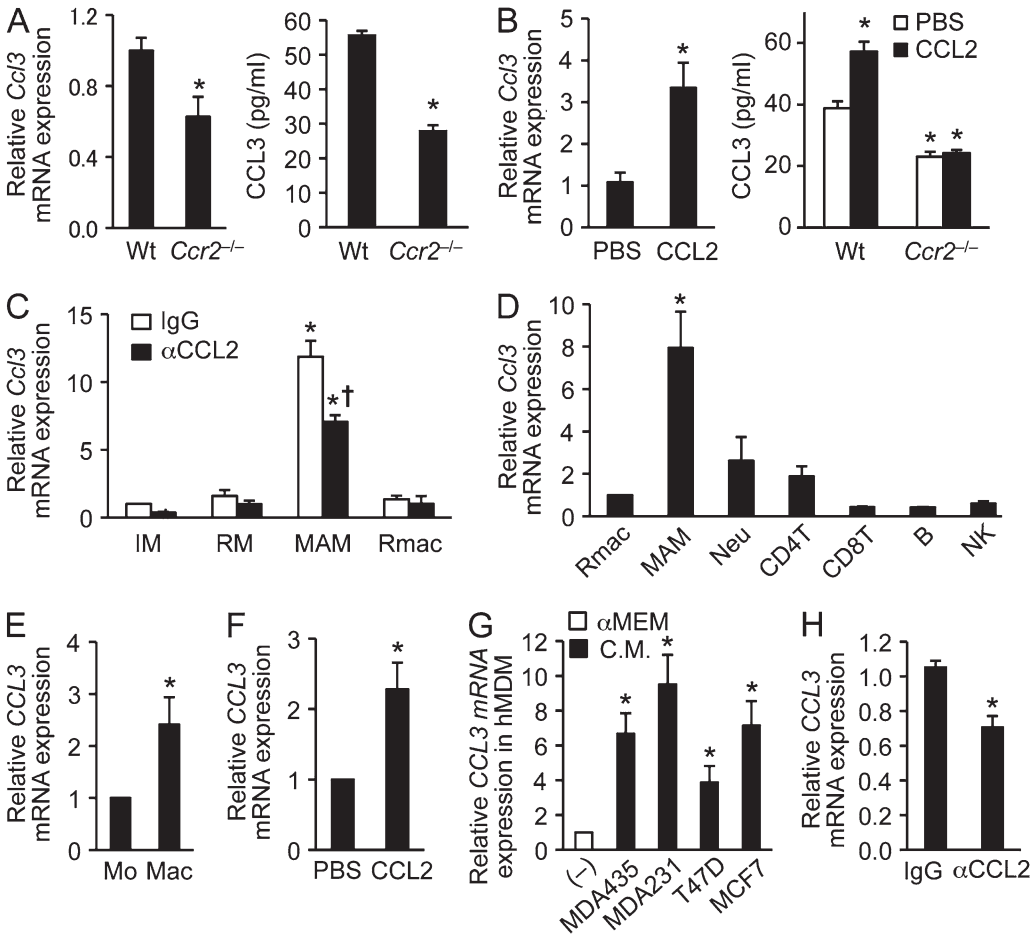

Figure 2. CCR2 signaling regulates CCL3 expression in MAMs. (A) Levels of *Ccl3* mRNA (left) and CCL3 protein (right) in BMDMs isolated from WT or *Ccr2*$^{-/-}$ mice were assessed by RT-PCR ($n = 6$ per genotype, 6 independent experiments) and ELISA ($n = 3$ per genotype, two independent experiments). Data are means ± SEM. *, $P < 0.01$ versus WT. (B) *Ccl3* mRNA (left) and CCL3 protein (right) were assessed by RT-PCR ($n = 3$, 2 independent experiments) and ELISA ($n = 3$ per genotype, 2 independent experiments) in macrophages cultured with PBS or recombinant CCL2 (100 ng/ml). The BMDMs were isolated from WT or *Ccr2*$^{-/-}$ mice. Data are means ± SEM. *, $P < 0.01$. (C) Expression of *Ccl3* mRNA was assessed by RT-PCR ($n = 4$, four independent experiments) in monocytes and macrophages obtained from E0771-LG tumor-injected mice treated with neutralizing anti-CCL2 or control IgG antibodies. IM, inflammatory monocytes (CD115$^+$CD11b$^+$Ly6C$^+$); RM, resident monocytes (CD115$^+$CD11b$^+$Ly6C$^-$); MAMs (F4/80$^+$CD11b$^+$CD11c$^-$Ly6C$^-$); Rmac, resident macrophages (F4/80$^+$CD11b$^-$CD11c$^+$Ly6C$^-$). Data are means ± SEM. *, $P < 0.01$ versus IgG-IM; †, $P < 0.05$ versus IgG-MAM. Gating strategies are shown Fig. S1. (D) Expression of *Ccl3* mRNA was assessed by RT-PCR in Rmac, MAM ($n = 7$, 7 independent experiments) or neutrophil (Neu), CD4$^+$ T cell, CD8$^+$ T cell, B cell, and NK cell ($n = 3$, 3 independent experiments). The leukocytes were isolated from tumor-bearing mouse lung. Data are means ± SEM. *, $P < 0.01$ versus Rmac. (E) Relative *CCL3* mRNA expression was assessed by RT-PCR ($n = 4$, 4 independent experiments) in human monocytes (Mo) and those differentiated into macrophages by CSF-1 (Mac). Data are means ± SEM. *, $P < 0.05$. (F) Relative *CCL3* mRNA level was assessed by RT-PCR ($n = 4$, 4 independent experiments) in human macrophages cultured with recombinant human CCL2 (100 ng/ml). Data are means ± SEM. *, $P < 0.05$. (G) Expression of *CCL3* mRNA was assessed by RT-PCR in human MDMs (hMDM) cultured with conditioned medium (C.M.) from human cancer cell lines as indicated. As a control (–), the cells were cultured in nonconditioned medium (αMEM including 10% FBS and 10^3 U/ml CSF-1). $n = 5$, 5 independent experiments. Data are means ± SEM. *, $P < 0.01$. (H) Expression of *CCL3* mRNA was assessed by RT-PCR in human macrophages cultured in MDA231 conditioned medium with neutralizing anti-CCL2 or control IgG antibodies. $n = 3$. Data are means ± SEM. *, $P < 0.05$.

and determined tumor loads in the lung by in vivo bioluminescence imaging. In support of our hypothesis, the spontaneous pulmonary metastases from the orthotopic 4175 tumors were markedly suppressed by *Ccl3* deficiency (Fig. 3 B). To confirm this result in a spontaneous tumor-developing GEM model, we introduced the *Ccl3*-null allele to the PyMT mice on a BL6 background and found that the number of lung metastasis foci was significantly lower in PyMT:*Ccl3*$^{-/-}$ than PyMT:*Ccl3*$^{+/+}$ mice (Fig. 3, C and D). As we could not find significant differences in the size of foci or weight of primary tumors (Fig. 3 D), CCL3 appears to be required for metastatic seeding of cancer cells rather than their growth at the primary and metastatic sites.

We thus investigated the role of CCL3 in extravasation, one of the rate-limiting steps of metastasis, using an experimental metastasis model that enables cancer cells to

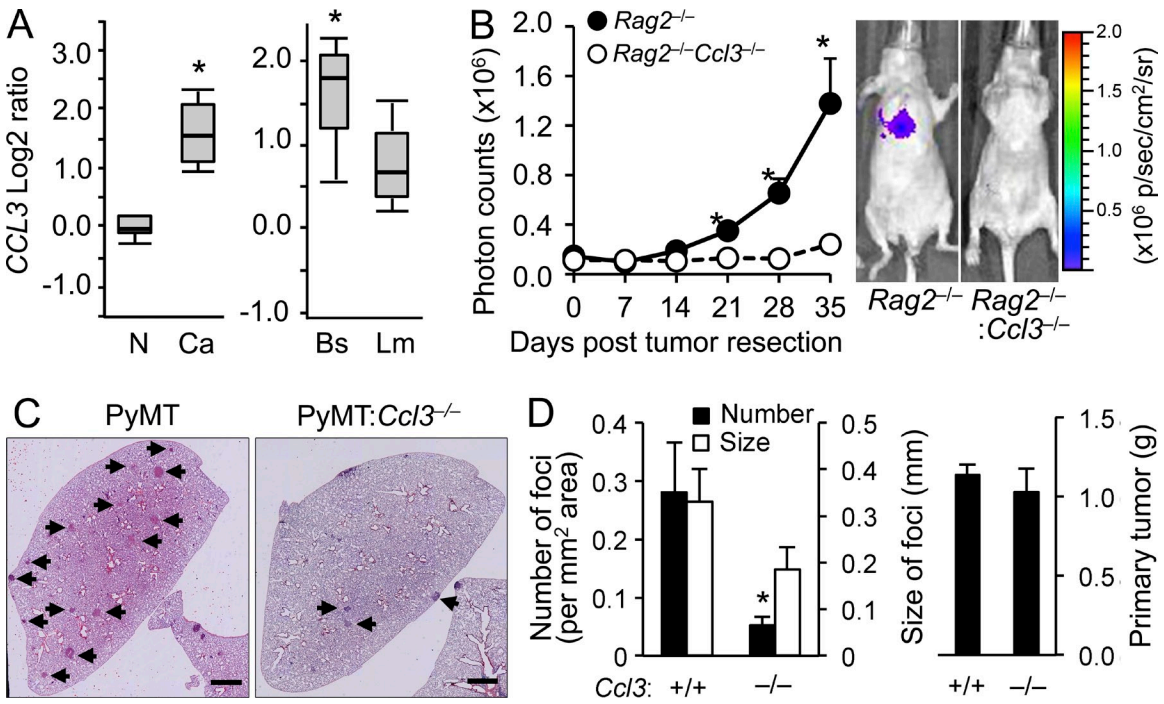

Figure 3. Loss of CCL3 in stromal cells suppresses pulmonary metastasis of human and mouse breast cancer cells. (A) Oncomine search results for CCL3 are shown. (left) *CCL3* transcript abundance in stroma of breast cancer (Ca) and normal tissue (N). P = 2.61 × 10^{-16}; fold change, 3.078. (right) *CCL3* levels in basal-like (Bs) and luminal-like (Lm) invasive breast carcinoma showing increase in basal cancers. P = 2.28 × 10^{-4}; fold change, 1.747. (B) Lung metastatic burden from orthotopic mammary tumors was quantified (n = 3/genotype, 3 independent experiments). The tumors were developed by MDA231:4175TGL human breast cancer cells in nude mice transplanted with *Rag2*$^{-/-}$ or *Ccl3*$^{-/-}$*Rag2*$^{-/-}$ BM cells. Plots show normalized photon flux in the lung over time. Data are means ± SEM. *, P < 0.05. Representative images of mice at 35 wk are shown (right). (C) Representative H&E stained microscopy images of the lung from PyMT (n = 8) and PyMT:*Ccl3*$^{-/-}$ (n = 7) mice with spontaneous metastatic foci (Arrowheads) are shown. Bars, 1 mm. (D) Number and size of lung metastatic foci (left) and primary tumor weights (right) were assessed in autochthonous PyMT (n = 8) or PyMT:*Ccl3*$^{-/-}$ mice (n = 7) at 27–30 wk of age (4 independent experiments). Data are means ± SEM. *, P < 0.01.

avoid the early metastatic steps from the primary tumor such as local invasion and intravasation. Namely, we injected E0771-LG cells into the tail vein of mice that received BM transplantation (BMT) from WT, *Ccl3*$^{-/-}$, or *Ccr2*$^{-/-}$ mice. Consistent with our other experimental models, transplantation of *Ccl3*$^{-/-}$ BM cells reduced number of foci without affecting the size of foci (Fig. 4 A). The suppressive effect of *Ccl3* gene ablation was comparable with that of *Ccr2* knockout. To investigate the requirement of CCL3 in lung metastasis of another cell line, we performed experimental metastasis assays with Met-1 mouse mammary tumor cells. Because the cells are derived from the PyMT tumor in FVB mice (Borowsky et al., 2005), we used anti-CCL3 neutralizing antibody instead of *Ccl3*$^{-/-}$ mice (C57BL/6). Consistent with the genetic model, pretreatment with anti-CCL3 antibody significantly suppressed the number of foci (Fig. 4 B). Although the suppressive effect of the antibody treatment was smaller than that of genetic *Ccl3* deletion, we are unable to compare the two models (Met-1 and E0771) in the null mutant because of the genetic background. The lower effect caused by the antibody treatment may also due to the very high dose of the antibody (ND_{50} = 5–25 µg/ml) required to achieve complete neutralization of CCL3 in mice that is greater than the amount of antibody available to us for this experiment. Nevertheless the effects were highly significant compared with the control antibody.

To investigate the contribution of MAMs to this CCL3-promoting metastasis, we performed adoptive transfer of IMs. We have reported that transferred IMs (CD11b^{+}Ly6C^{high}) are readily detectable in the tumor-challenged lung at least 5 d after transfer, and a significant portion of them have differentiated into MAMs (CD11b^{+}Ly6C^{lo}) within 2 d (Qian et al., 2011). We have also shown that intravenously injected cancer cells extravasate within 2 d after injection and this seeding is suppressed by macrophage depletion (Qian et al., 2009), suggesting that IMs injected with cancer cells can differentiate to MAMs and support tumor metastasis. We thus injected IMs isolated from WT (*Ccl3*$^{+/+}$) or *Ccl3*$^{-/-}$ mice in combination with cancer cells to the mice transplanted with *Ccl3*$^{-/-}$ BM cells (BMT:*Ccl3*$^{-/-}$). Importantly, the suppressive effect on foci numbers in the BMT:*Ccl3*$^{-/-}$ mice was significantly rescued by the one-time injection of *Ccl3*$^{+/+}$ IMs (Fig. 4 C). In contrast, adoptive transfer of *Ccl3*$^{-/-}$ IMs did not change the number of foci. Because MAMs originate from IMs (Qian

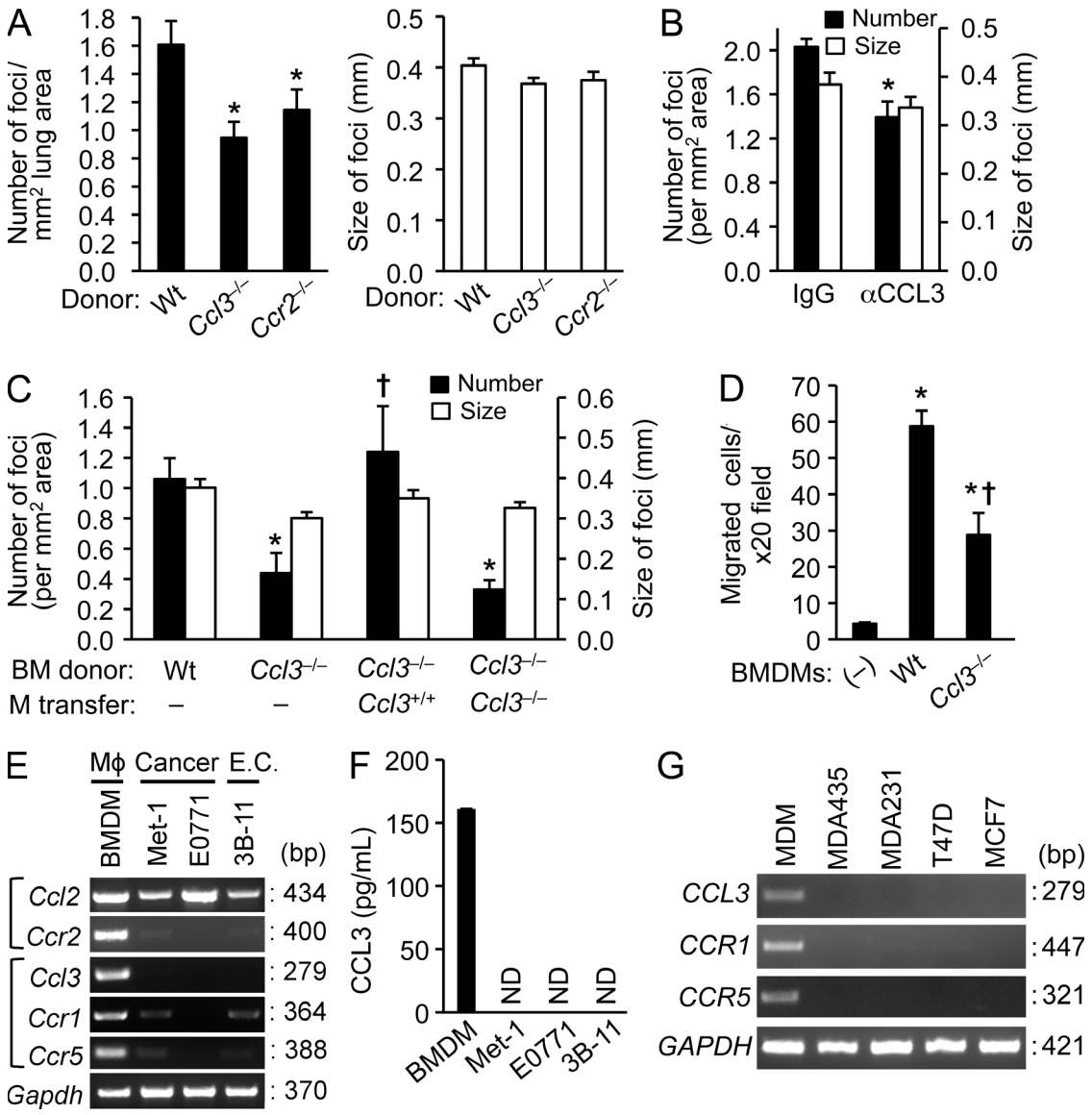

Figure 4. Expression of CCL3 in MAMs promotes metastatic seeding of cancer cells. (A) Number and size of lung foci were assessed in WT irradiated mice transplanted with BM cells from C57BL/6 (WT, $n = 13$), *Ccl3*$^{-/-}$ ($n = 14$), or *Ccr2*$^{-/-}$ ($n = 15$) mice (three independent experiments). After reconstitution of their BM, mice were injected with E0771-LG cells and euthanized after 11 d. Data are means ± SEM. *, $P < 0.01$ versus WT. (B) Number and size of lung foci were assessed in FVB mice injected with Met-1 cells (three independent experiments). Mice were treated with IgG ($n = 9$) or anti-CCL3 antibodies ($n = 6$) 24 and 2 h before tumor injection. Data are means ± SEM. *, $P < 0.01$. (C) Number and size of lung foci were assessed at day 11 after E0771-LG tumor cell injection in mice transplanted with WT ($n = 8$) or *Ccl3*$^{-/-}$ ($n = 7$) BM. The *Ccl3*$^{-/-}$ BM transplanted mice were also injected with WT (*Ccl3*$^{+/+}$, $n = 7$) or *Ccl3*$^{-/-}$ ($n = 6$) inflammatory monocytes (IMs). Data are means ± SEM from four independent experiments. *, $P < 0.01$ versus WT; †, $P < 0.05$ versus *Ccl3*$^{-/-}$. (D) Number of transmigrated E0771-LG cells was measured in the transendothelial migration assay in the absence (–) or presence of BMDMs from C57BL/6 or *Ccl3*$^{-/-}$ mice ($n = 3$, 2 independent experiments). Mean cell number in each insert was determined by the counts from five fields. Data are means ± SEM. *, $P < 0.05$ versus BMM (–); †, $P < 0.01$ versus WT. (E) mRNA expression of CC-chemokine ligands and their receptors in cultured mouse macrophages (BMDM), cancer cells (Met-1 and E0771), and endothelial cells (3B-11), as indicated (two independent experiments). PCR product size (bp) is shown on the right. (F) Secretion of CCL3 protein was assessed by ELISA in cultured mouse macrophages (BMDM), cancer cells (Met-1 and E0771), and endothelial cells (3B-11), as indicated ($n = 3$, three independent experiments). ND, not detected. (G) mRNA expression of CCL3 and its receptors in cultured human macrophages (MDM) and breast cancer cell lines (two independent experiments). PCR product size (bp) is shown on the right.

et al., 2011) and are the major source of CCL3 in the metastasis sites (Fig. 2 D), these results collectively indicate that CCL3 from MAMs can promote metastatic seeding of breast cancer cells. Supporting this interpretation, in vitro extravasation of cancer cells, which was promoted by WT macrophages, was significantly suppressed by *Ccl3* deficiency (Fig. 4 D). It is

noteworthy that only the macrophages expressed *Ccr2* and *Ccl3* in this in vitro system (Fig. 4, E–G), suggesting that macrophages are the cells that respond to CCL2 signaling and produce CCL3.

CCL3–CCR1 axis enhances MAM accumulation and promotes tumor metastasis

Because mRNA of the CCL3 receptors CCR1 and CCR5 are expressed predominantly by human and mouse macrophages rather than breast cancer cells or endothelial cells (Fig. 4, E–G; see also Fig. 6 H), the MAM-derived CCL3 is likely to act as an autocrine mediator for MAMs rather than increasing cancer cell motility/invasiveness or vascular permeability. In the experimental metastasis model, we have shown that the MAMs ($CD11b^+$) are recruited to the lung as early as 36 h after introduction of cancer cells into circulation. Using an ex vivo imaging system, we have also shown that majority of the i.v. injected cancer cells directly contact with the MAMs and extravasate within 48 h. In this system, macrophage depletion markedly delays the tumor cell extravasation (Qian et al., 2009). We therefore hypothesized that MAM-derived CCL3 may promote metastatic seeding by enhancing the early accumulation of MAMs in tumor cell challenged lungs. To test this hypothesis, we determined the number of $CD11b^+$ macrophages in the lung from WT or *Ccl3*$^{-/-}$ mice 24 h after tumor injection. Consistent with our previous results (Qian et al., 2009), the number of $CD11b^+$ macrophages was very low in the normal lung of WT mice and was increased by tumor injection by 24 h (Fig. 5 A and Fig. S1). However, such an accumulation did not occur in *Ccl3*$^{-/-}$ mice (Fig. 5 A), suggesting that CCL3 is required for MAMs to accumulate at the metastasis sites. Although *Ccr2* deficiency suppressed MAM accumulation, it also suppressed basal levels of CD11b-positive cells and circulating monocytes (Fig. 5 A), consistent with the role for the CCL2–CCR2 axis regulating monocyte emigration from the BM (Serbina et al., 2008). In contrast, loss of *Ccl3* did not alter the steady-state numbers of MAMs or monocytes (Fig. 5 A). Furthermore, *Ccl3* deficiency did not reduce the numbers of resident macrophages, neutrophils, or lymphocytes (Fig. 5 B). Although tumor injection increased neutrophil accumulation in the lung of WT mice, this was independent of CCL3. Nevertheless, we investigated whether there is a contribution of neutrophils to metastatic seeding by depleting them via anti-Ly6G antibodies treatments (Fig. 5 C). To deplete neutrophils during metastatic seeding, we treated mice with antibodies 24 and 5 h before, and 16 h after tumor injection, as most i.v. injected cancer cells complete extravasation within 48 h (Qian et al., 2009) and the suppressive effect of a single antibody injection lasts at least 2 d (Cain et al., 2011). We found that the anti-Ly6G depletion of neutrophils did not alter the numbers of lung metastatic foci (Fig. 5 D). In contrast, depletion of the MAM progenitor IMs significantly suppressed lung metastasis of cancer cells (Fig. 5, E and F). To establish this, we used rtTA:tetO-Cre:*Csf1r*$^{F/F}$ mice treated with doxycycline (Dox), in which loss of functional CSF-1 receptor significantly ablated circulating IMs (Fig. 5 E) and reduced the number of metastatic foci (Fig. 5 F). As a control administration of Dox alone did not affect the number of metastasis foci (Control, 0.41 ± 0.1; Dox treated, $0.52 \pm 0.2/mm^2$ lung area), these results indicate that CCL3 promotes metastatic seeding of cancer cells by promoting the early accumulation of IM/MAMs.

CCR1 and CCR5 are the only known cognate receptors of CCL3 (Schall and Proudfoot, 2011). To determine their contributions to the early MAM accumulation, we first confirmed that MAMs expressed CCR1 and CCR5 (Fig. 6 A). Interestingly, MAMs expressed higher levels of *Ccr1* and *Ccr5* mRNA and protein than circulating IMs (Fig. 6, A and B). In contrast, CCR2 is expressed higher on IMs than MAMs (Fig. 6 A). Consistent with our in vitro data (Fig. 4 E), $CD45^-$ $CD31^+$ endothelial cells in the tumor-challenged lung or E0771 cancer cells did not express CCR1 or CCR5 (Fig. 6, C and D). Next we determined the number of $CD11b^+$ macrophages in the lungs of WT, *Ccr1*$^{-/-}$, or *Ccr5*$^{-/-}$ mice 24 h after tumor-cell injection. Consistent with our previous results (Qian et al., 2009; Fig. 5 A), tumor-injected WT mice showed 70% increase in number of MAMs compared with normal mice. Such increase was significantly reduced in *Ccr1*$^{-/-}$ mice whereas the number of IMs were not changed (Fig. 6 E). In contrast, loss of *Ccr5* did not suppress the MAM accumulation (Fig. 6 E), suggesting that it is the CCL3–CCR1 axis that is required for early accumulation of MAMs. Loss of *Ccr1* also suppressed the number of metastatic foci and the ability of macrophages to promote in vitro extravasation of breast cancer cells (Fig. 6, F and G). In the in vitro extravasation assay, macrophages are the only cell type that expresses CCR1 and it is not expressed by cancer (E0771 or Met-1) or endothelial (3B-11) cells (Fig. 6, D and H). Collectively, these results show that the MAM-derived CCL3 mainly acts as an autocrine mediator and that the MAM accumulation through CCL3–CCR1 axis is involved in promotion of cancer cell extravasation.

CCR1 signaling prolongs retention of MAMs at metastasis sites by enhancing MAM–cancer cell interaction

To investigate how CCR1 promotes MAM accumulation, we injected WT or *Ccr1*$^{-/-}$ IMs labeled with CMFDA fluorescent dye into mice bearing similar lung metastatic loads and followed their fate up to 42 h after transfer. Labeled monocytes from both genotypes infiltrated into the lung to a similar extent after 18 h. By 42 h, however, there were significantly fewer *Ccr1*$^{-/-}$ cells than WT cells (Fig. 7 A). While the ratio of $CMFDA^+$ cells in the MAM population, which indicates differentiation of IMs ($CD11b^+Ly6c^+$) to MAMs ($CD11b^+Ly6c^-$), increased by 42 h, there was no difference between WT and *Ccr1*$^{-/-}$ mice (Fig. 7 B). These results indicate that activation of CCR1 signaling promotes retention of MAMs in the metastatic lung, but not the recruitment or differentiation of IMs.

Because most cancer cells extravasate within 48 h after injection and interact with MAMs in the lung (Qian et al., 2009), we hypothesized that the CCL3–CCR1 axis might

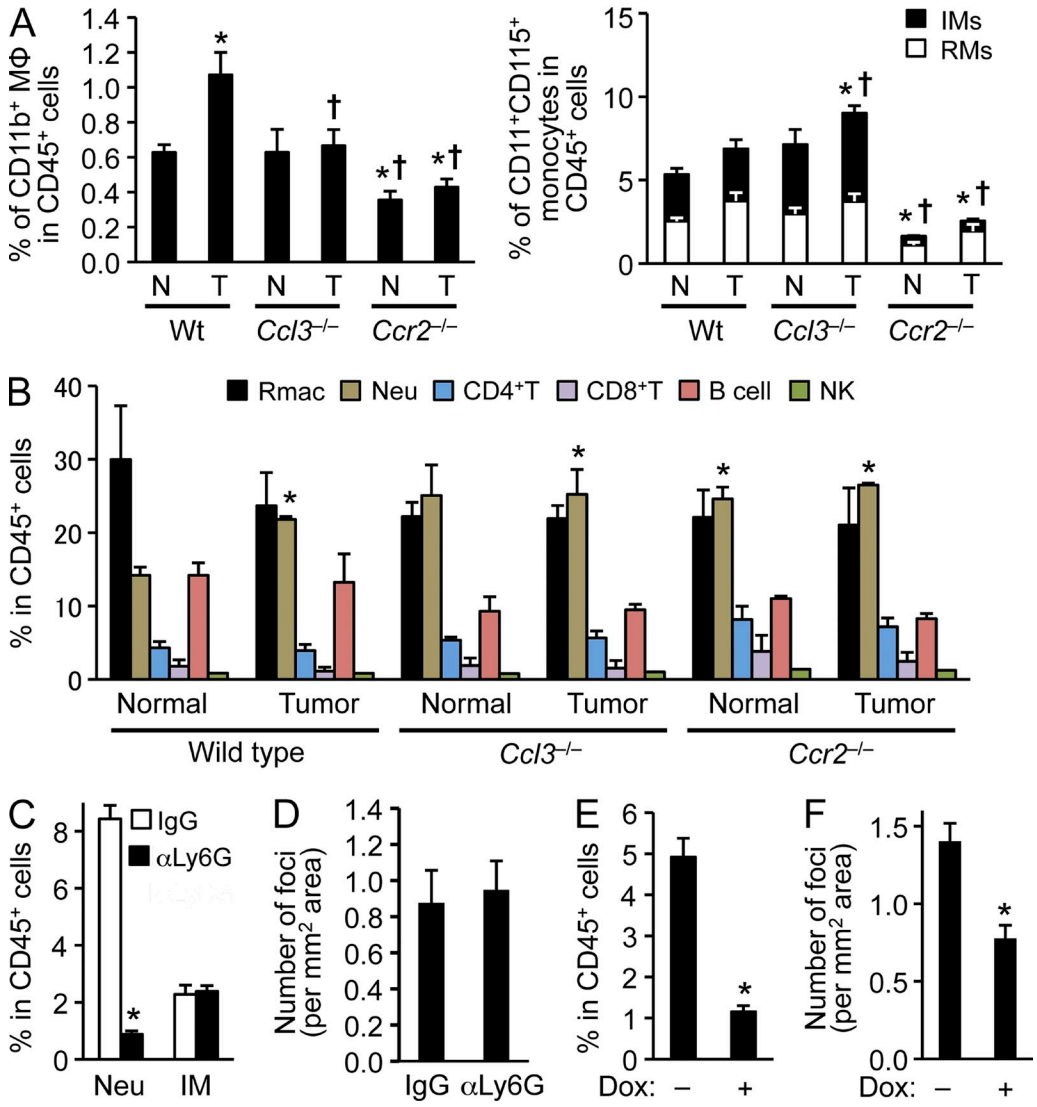

Figure 5. CCL3 is required for MAMs to accumulate in tumor-challenged lung. (A) Relative numbers of lung CD11b$^+$ macrophages (left) or circulating CD11b$^+$CD115$^+$ monocytes (right) in C57BL/6 (WT; $n = 14$), *Ccl3*$^{-/-}$ ($n = 4$), and *Ccr2*$^{-/-}$ ($n = 4$) mice (normal; N) were compared with those i.v. injected with E0771-LG cells 24 h before measurement (tumor; T). IM, inflammatory monocytes (Ly6C$^+$); RM, resident monocytes (Ly6C$^-$). Data are measured as percentage of macrophages or monocytes in CD45$^+$ cells (at least four independent experiments). Data are means ± SEM. *, $P < 0.05$ versus WT-N; †, $P < 0.05$ versus WT-T. Gating strategy is shown in Fig. S1. (B) Relative numbers of leukocytes in lungs of C57BL/6 (WT; $n = 14$), *Ccl3*$^{-/-}$ ($n = 4$), and *Ccr2*$^{-/-}$ ($n = 4$) mice are shown. Mice were injected with PBS (Normal) or E0771-LG cells (Tumor) 24 h before measurement. Rmac, resident macrophages; Neu, neutrophils. Data are measured as percentage of macrophages or monocytes in CD45$^+$ cells (at least four independent experiments) and shown as means ± SEM. *, $P < 0.05$ versus WT-Normal. (C) Relative numbers of circulating neutrophils (Neu) and inflammatory monocytes (IM) in WT mice 24 h after 2 d of treatment with anti-Ly6G antibody ($n = 5$, two independent experiments). Data are measured as percentage of macrophages or monocytes in CD45$^+$ cells. Data are means ± SEM. *, $P < 0.01$. (D) Number of lung foci was assessed in neutrophil depleted WT mice at day 11 after E0771-LG breast cancer cell injection. Mice were treated with IgG or anti-Ly6G antibodies 24 or 5 h before, and 16 h after tumor cell injection ($n = 4$, four independent experiments). Data are means ± SEM. No statistical significance was observed. (E) Relative number of circulating monocytes was assessed in rtTA:tetO-Cre:*Csf1r*$^{F/F}$ mice treated with or without doxycycline (Dox) in drinking water for 7 d ($n = 4$, 2 independent experiments). Data are means ± SEM. *, $P < 0.01$. (F) Number of metastasis foci was assessed in monocyte-depleted rtTA:tetO-Cre:*Csf1r*$^{F/F}$ mice at day 11 post-tumor injection. The rtTA:tetO-Cre:*Csf1r*$^{F/F}$ mice injected with E0771-LG cells were given water with or without doxycycline (Dox) in drinking water from 7 d before tumor injection to the endpoint ($n = 7$, 2 independent experiments). Data are means ± SEM. *, $P < 0.01$.

enhance MAM retention through regulating the interaction between cancer cells and MAMs. Supporting this hypothesis, loss of *Ccl3* or *Ccr1* reduced the numbers of CD11b$^+$ cells interacting with disseminating cancer cells in the lung (Fig. 7, C and D). We then determined the duration of interaction between macrophages and E0771-LG cancer cells in vitro. We cultured macrophages labeled with CMTMR fluorescent dye on Matrigel with cancer cells and tracked them for

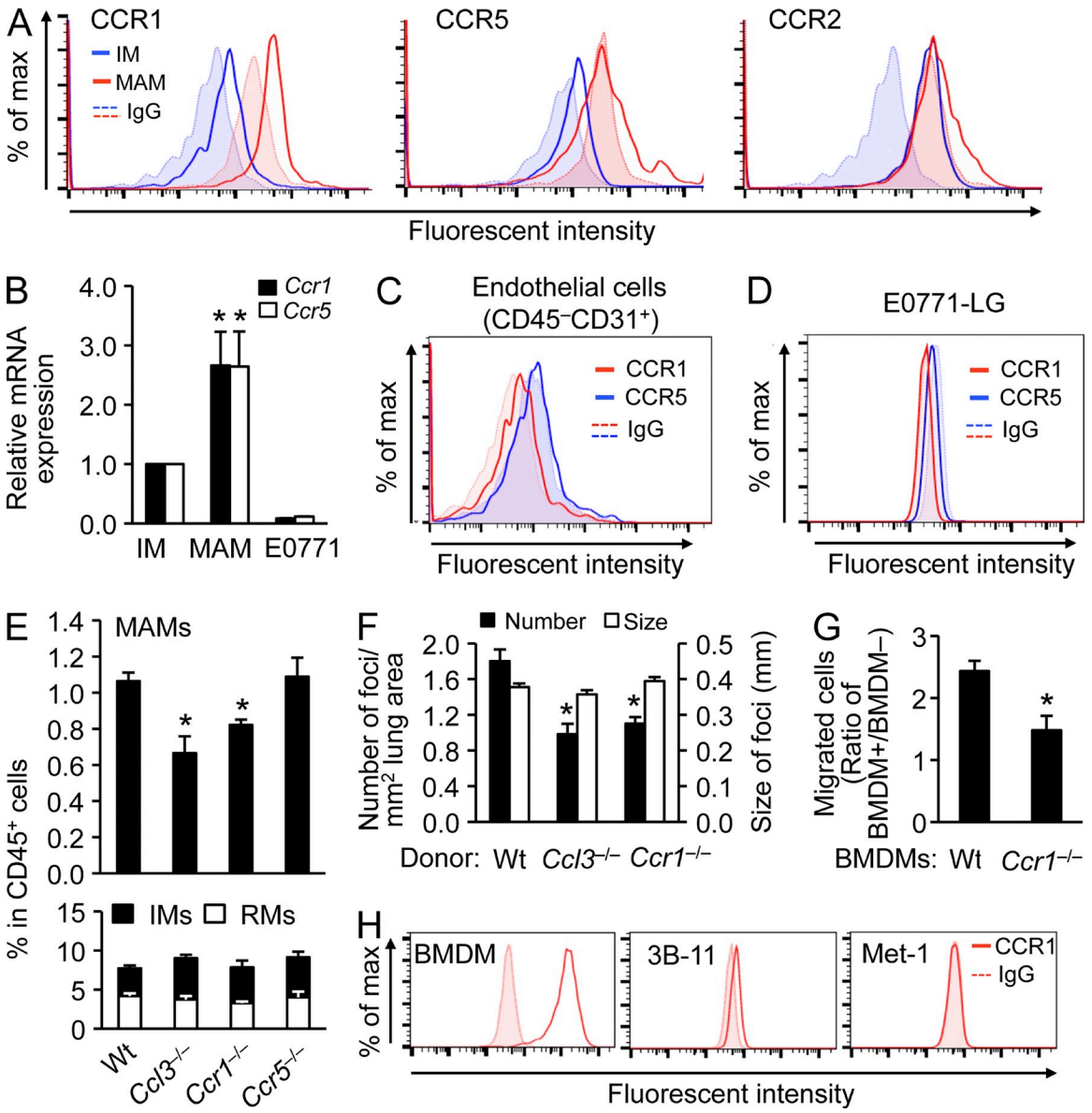

Figure 6. The CCL3–CCR1 axis is required for accumulation of MAMs and after extravasation of cancer cells. (A) Levels of chemokine receptors were assessed by flow cytometry in circulating inflammatory monocytes (IMs) and lung MAMs, as indicated. Cells were isolated from WT mice 24 h after E0771-LG tumor cell injection ($n = 3$). Dotted lines and shaded areas show control isotype matched IgG for each cell type. Representative histograms from three independent experiments are shown. (B) Levels of *Ccr1* and *Ccr5* mRNA were assessed in IMs, MAMs, and E0771-LG cancer cells. Cells were isolated from WT mice 24 h after E0771-LG tumor cell injection ($n = 4$). Data are means ± SEM. *, $P < 0.05$ versus IM. (C) Levels of chemokine receptors were assessed in $CD45^{-}CD31^{+}$ endothelial cells from the tumor cell–challenged lung. Cells were isolated from WT mice 24 h after E0771-LG tumor cell injection ($n = 3$). Dotted lines and shaded area show control isotype matched IgG for each receptor. A representative histogram from two independent experiments is shown. (D) Levels of chemokine receptors on cultured E0771-LG tumor cells were assessed by flow cytometry. Dotted lines and shaded areas show control isotype matched IgG for each receptor. A representative histogram from two independent experiments is shown ($n = 2$). (E) Relative numbers of lung $CD11b^{+}$ macrophages (top) and circulating $CD11b^{+}CD115^{+}$ monocytes (bottom) were assessed by flow cytometry in C57BL/6 (WT; $n = 14$), *Ccl3*$^{-/-}$ ($n = 4$), *Ccr1*$^{-/-}$ ($n = 7$), and *Ccr5*$^{-/-}$ ($n = 7$) mice challenged with E0771-LG cells 24 h before measurement (at least two independent experiments/genotype). Data are means ± SEM. *, $P < 0.05$ versus WT. (F) Number and size of lung foci were assessed in mice transplanted with BM cells from C57BL/6 (WT, $n = 14$), *Ccl3*$^{-/-}$ ($n = 11$), or *Ccr1*$^{-/-}$ ($n = 9$) mice. Mice were injected with E0771-LG cells (two independent experiments). Data are means ± SEM. *, $P < 0.01$. (G) Number of transmigrated E0771-LG cells was measured in the transendothelial migration assay in the presence of BMDMs from C57BL/6 or *Ccr1*$^{-/-}$ mice ($n = 6$, three independent experiments). Mean cell number in each insert was determined by the counts from five fields. Data are means ± SEM. *, $P < 0.01$. (H) CCR1 protein expression was assessed by flow cytometry in BMDMs, 3B-11 endothlial cells, and Met-1 tumor cells. A representative histogram from two independent experiments is shown ($n = 2$).

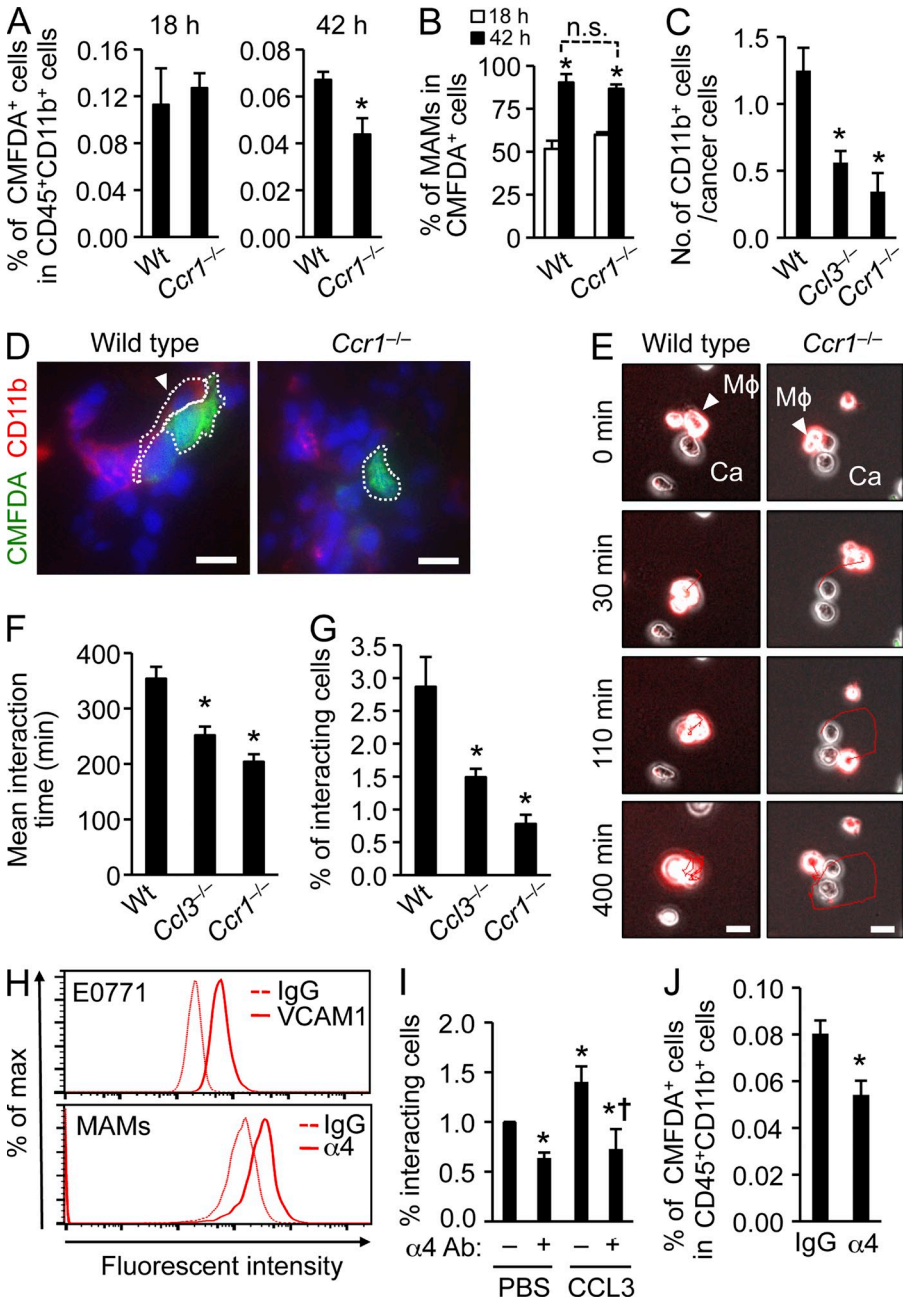

Figure 7. CCR1 signaling enhances attachment of macrophages to cancer cells and promotes their retention in tumor-bearing lung. (A) The fate of transferred CMFDA-labeled IMs in mouse lung metastases were followed. $CD11b^+CD115^+Ly6C^+$ inflammatory monocytes (IMs) isolated from WT or *Ccr1*$^{-/-}$ mice were labeled with CMFDA and transferred to WT mice that received i.v. injection of E0771-LG cells expressing luciferase. Pulmonary tumor burdens in the recipients were determined by in vivo bioluminescence imaging 1 d before monocyte transfer (10 d after tumor injection). Relative numbers of CMFDA-labeled cells in $CD45^+CD11b^+$ cells from tumor bearing lungs were assessed 18 or 42 h after IM transfer ($n = 4$, 4 independent experiments). Data are means ± SEM. *, $P < 0.01$. (B) Data show percentage of $F4/80^+CD11b^+Ly6C^-$ cells (MAMs) in $CMFDA^+$ cells from tumor bearing lung ($n = 4$, 4 independent experiments). Data are means ± SEM. *, $P < 0.01$ versus 18 h. n.s., not significant. (C) Number of $CD11b^+$ cells associated with cancer cells in the lung were counted in WT *Ccl3*$^{-/-}$, and *Ccr1*$^{-/-}$ mice from images in D ($n = 4$, 4 independent experiments). Interaction between cancer cells and $CD11b^+$ myeloid cells were detected by immunostaining 24 h after intravenous injection of CMFDA-labeled E0771-LG cells. Data are means ± SEM. *, $P < 0.05$. (D) Representative fluorescence microscopy images of lung 24 h after E0771-LG injection. Green, CMFDA-labeled E0771-LG cells; Red, CD11b; Blue, nuclei; Arrow head, interaction between myeloid cells and cancer cells. Dotted line indicates the interaction between macrophage and tumor cell. Bars, 10 µm. (E) Interactions between macrophages and cancer cells ($n = 3$, 3 independent experiments) were assessed by time-lapse imaging. Representative microscopy images over a 400-min time course are shown. The time when the target macrophage attached to cancer cells was designated as 0 min. Arrow head, the target macrophage (Mφ) attached to the cancer cell (Ca); Red line, track of macrophage. Bars, 10 µm. See Videos 1 and 2. (F) Mean duration of interactions between macrophages and cancer cells ($n = 3$, three independent experiments) were assessed from images in (E; 10 fields/group in each experiment). Data are means ± SEM. *, $P < 0.01$. (G) Interactions between macrophages and cancer cells were assessed by flow cytometry ($n = 4$, 4 independent experiments). BMDMs from C57BL/6, *Ccl3*$^{-/-}$, and *Ccr1*$^{-/-}$ mice were labeled with CMTMR and mixed with CMFDA-labeled E0771-LG cells. Data are represented as the ratio of CMFTMR/CMFDA double-positive population. Data are means ± SEM. *, $P < 0.05$. (H) Surface levels of VCAM-1 on E0771-LG tumor cells and integrin α4 on MAMs isolated from lungs 24 h after tumor injection were assessed by flow cytometry. Representative results from two independent experiments ($n = 2$) are shown. (I) Interactions between macrophages and cancer cells in the presence of recombinant CCL3 or PBS were assessed by flow cytometry ($n = 4$, four independent experiments). Macrophages were pretreated with anti-integrin α4 neutralizing antibody (α4 Ab: +) or control isotype matched IgG (α4 Ab: –). Data are means ± SEM. *, $P < 0.01$ versus PBS; †, $P < 0.05$ versus CCL3. (J) The effect of integrin α4 inhibition on the fate of transferred IMs in mouse lung metastases was assessed by flow cytometry following the experimental procedure in A. Anti-integrin α4 neutralizing antibody (α4) was injected 18 h after IM transfer. Relative numbers of CMFDA-labeled cells in $CD45^+CD11b^+$ cells from tumor bearing lung were assessed 42 h after IM transfer ($n = 5$, five independent experiments). Data are means ± SEM. *, $P < 0.05$.

24 h by microscopy. The majority of WT macrophages were retained at the same position once they attached to cancer cells, and the mean interaction time was 353 ± 21 min (Fig. 7, E and F). In contrast, *Ccl3*$^{-/-}$ or *Ccr1*$^{-/-}$ macrophages interacted with cancer cells for a significantly shorter time than WT macrophages (252 ± 16 or 204 ± 14 min, respectively; Fig. 7 F). We also found that *Ccl3*$^{-/-}$ or *Ccr1*$^{-/-}$ macrophages more frequently detached from cancer cells and moved around the dish (Fig. 7 E and Videos 1 and 2), suggesting that the CCL3–CCR1 axis can enhance macrophage–cancer cell interaction, which arrests the macrophages. To confirm these results, we cultured macrophages with E0771-LG cancer cells together in suspension for 1 h, and determined the ratio of macrophages interacting with cancer cells by flow cytometry. Consistent with our findings (Fig. 7, E and F), we found a lower number of *Ccl3*$^{-/-}$ or *Ccr1*$^{-/-}$ macrophages bound to cancer cells compared with WT macrophages (Fig. 7 G).

A recent report indicates that human breast cancer cells expressing VCAM-1 can bind to leukocytes that express α4 integrin, a VCAM-1 receptor (Chen et al., 2011). Because E0771-LG mouse breast cancer cells also expressed VCAM-1 and MAMs accumulated in the tumor-bearing lung expressed α4 integrin (Fig. 7 H), we investigated the possibility that the CCL3–CCR1 axis promotes macrophages to interact with cancer cells through α4 integrin. The interaction between macrophages and cancer cells was enhanced by CCL3 in *Ccl3*$^{-/-}$ macrophages, and suppressed by anti-α4 integrin antibody treatment (Fig. 7 I). The antibody treatment also suppressed macrophage-cancer cell interaction in the absence of CCL3 to the comparable level with that in the presence of CCL3, suggesting that α4 integrin is required for both basal as well as CCL3-induced macrophage attachment to cancer cells. Furthermore, treatment of tumor-bearing mice with anti-α4 integrin antibody 18 h after IM transfer, a time point when the highest number of IMs had infiltrated into the lung (Fig. 7 A), resulted in significantly reduced numbers of transferred cells after 42 h (Fig. 7 J). This result indicates that α4 integrin contributes to MAM retention in vivo.

Collectively, our results in several models of metastasis including spontaneous GEM ones revealed the existence of a chemokine cascade that promotes breast cancer metastasis. Activation of CCL2–CCR2 signaling promotes CCL3 secretion that activates CCR1 signaling in MAMs. Activation of CCR1 in turn enhances interaction of MAMs with metastasizing cancer cells at least in part through integrin α4. As a result, prolonged MAM retention enhances extravasation of cancer cells and therefore metastasis.

DISCUSSION

Previously, we showed that a chemokine CCL2 recruits IMs to metastatic sites where they differentiate to MAMs (Qian et al., 2011). In this study, we revealed a novel role for CCL2 as a trigger of a prometastatic chemokine cascade involving CCL3 signaling via CCR1 that is required for efficient metastasis. These data illustrate a signaling relay that amplifies the pathology already in the system by promoting retention of recruited monocytes that stimulate tumor cell establishment at the metastatic site.

Our in vivo and in vitro results indicate that CCL2 can increase CCL3 expression in MAMs at the metastasis site. The CCL2-induced CCL3 expression is likely to be specific to the prometastatic macrophage lineage, as neutralization of CCL2 by antibodies significantly reduced *Ccl3* expression in IMs and MAMs, but not in resident monocytes or macrophages. Consistent with this interpretation, expression of *Ccl3* was highest in MAMs compared with other leukocytes in the tumor-bearing lung. Importantly, a single injection of *Ccl3*$^{+/+}$ IMs but not IMs lacking CCL3 was sufficient to rescue the suppressive effect of *Ccl3*$^{-/-}$ on experimental metastasis. Furthermore, in our in vitro extravasation assay, macrophages but not cancer cells or endothelial cells secrete CCL3 protein. These findings strongly suggest that MAMs are the main cell type in the metastasis site that produces CCL3 in response to CCL2 signaling. In cultured macrophages, basal CCL3 secretion is suppressed by *Ccr2* deficiency, suggesting that CCL2 from macrophages cell autonomously regulates their CCL3 expression. Furthermore, *CCL3* expression is increased by conditioned medium from cancer cells in part through a CCL2-mediated mechanism. These results suggest that CCL2 secreted by both cancer cells and macrophages can promote secretion of CCL3 that is required for tumor metastasis. Consistent with this, we have reported that both cancer cells and macrophages express *Ccl2* mRNA, and that CCL2 from both tumor cells and stromal cells contribute to metastatic seeding of cancer cells (Qian et al., 2011). Our results, however, do not exclude the involvement of other factors in regulation of CCL3 secretion. However, identification of such molecules is beyond a scope of this study and requires further experimentation.

A recent study demonstrates that tumor-associated macrophages (TAMs) in the PyMT mammary tumors also express CCR2 and are differentiated from the IMs (Franklin et al., 2014). We have reported that the TAMs in the PyMT tumors also express high level of CCL3 (Ojalvo et al., 2009), suggesting that CCL2 regulates CCL3 expression in the TAMs as well. However, it will not affect the recruitment of MAMs to the lung as they originate from circulating monocytes (IMs) that preferentially migrate to the lung with metastatic tumors than to the primary mammary tumors through CCL2-mediated mechanism (Qian et al., 2011). Indeed, in the current study, we found only an inhibition of metastasis but no deficit in PyMT primary tumor growth in the absence of *Ccl3*. In contrast to our results, i.v. injected B16 melanoma cells develop more lung metastatic foci in *Ccl2*$^{-/-}$ or *Ccl3*$^{-/-}$ mice than WT mice (Nakasone et al., 2012). This discrepancy can be explained by a difference in the immune cell profile in particular cancer models. Namely, stromal loss of *Ccl3* or *Ccl2* reduces numbers of antitumorigenic immune cells such as CD4^{+} T, CD8^{+} T, and NK cells in the lung of melanoma metastasis model, but their numbers were not altered in the lung of our breast cancer metastasis model (Fig. 5 B). In contrast,

recruitment of prometastatic CD11b$^+$ MAMs is reduced by lack of stromal CCL2 or CCL3 in breast cancer models (Fig. 5 A; Qian et al., 2011) but not in the melanoma model. It remains to be clarified how different metastatic environments regulate the response of immune cells to CCL2/CCL3.

To our knowledge, this is the first report demonstrating the involvement of a chemokine cascade in metastasis. Although chemokine-induced chemokine expression is reported in cultured mouse dendritic cells (Fischer et al., 2001) and astrocytes (Luo et al., 2000), its contribution to tumor progression remains unknown. In our metastasis models using mouse and human cells, loss of CCL3 reduced early accumulation of MAMs in the tumor-challenged lung without affecting recruitments of neutrophils or lymphocytes. Interestingly, pulmonary infection with *C. neoformans* can induce CCL3 expression, and neutralization of CCL2 significantly decreases its levels in the lung of infected mice (Huffnagle et al., 1997). In this model, neutralization of CCL3 attenuated the accumulation of macrophages but not lymphocytes, suggesting that CCL2-induced CCL3 expression may be a common mechanism for macrophages to accumulate in the lung under pathological situations. Our results suggest that accumulation of macrophages (MAMs) via CCL2-induced CCL3 is required for the efficient metastatic seeding of cancer cells. Although we also found the early recruitment of neutrophils to the tumor-challenged lung by CCL3-independent mechanisms, they play a minor role in metastatic seeding, at least in our model. However, our results do not exclude their contributions to the establishment of metastatic foci as we treated the animals with neutralizing antibodies for a short time and did not assess the effects of prolonged treatment. In addition, neutrophils may well be important in cancer models other than breast cancer.

CCL3 can bind to CCR1 and CCR5 with high affinity. In our experimental metastasis model of breast cancer, loss of *Ccr1* but not *Ccr5* reduced early accumulation of MAMs that was observed by 24 h after tumor cell injection. In a lung metastasis model of renal cancer, however, loss of *Ccr5* but not *Ccr1* reduces macrophage accumulation in the lung foci after 7 d of tumor cell injection (Wu et al., 2008). These differences might suggest specialized requirement of chemokine receptors for macrophages to accumulate in distinct microenvironments at different phases of metastasis, i.e., CCR1 in early and CCR5 in late metastatic foci. Such nonredundant roles of CCR1 and CCR5 in myeloid cell accumulation have been demonstrated in some in vivo experiments using gene-ablated mice. For example, CCR1 but not CCR5 is required for macrophages to accumulate in the kidney of mice that have received unilateral ureteral obstruction (Eis et al., 2004). Furthermore, intraperitoneal CCL3 injection increases the number of neutrophils in the peritoneal cavity within 4 h and this accumulation is suppressed in *Ccr1*$^{-/-}$ but not in *Ccr5*$^{-/-}$ mice (Ramos et al., 2005). Interestingly, an in vitro migration assay shows that CCR1 predominantly mediates the arrest of monocytes under shear flow (Weber et al., 2001), which is consistent with our finding that CCR1 predominately contributes to the retention of IMs/MAMs. Thus, tumor cells may have subverted the normal cellular physiology of mononuclear phagocytes during infection or repair to their own survival advantage.

Although some studies show that CCL3 can stimulate in vitro migration of cancer cells (Youngs et al., 1997; Prest et al., 1999), we did not find expression of *Ccr1* or *Ccr5* in cancer cells. In contrast, we found that MAMs in the metastasis sites express both receptors, and *Ccr1/5* mRNA levels are much higher in the MAMs than circulating monocytes. Consistent with our results, freshly isolated human monocytes increase surface expression of CCR1 and CCR5 when they are kept in culture and differentiate to macrophages (Kaufmann et al., 2001). On the other hand, CCR2 expression is reduced in macrophages compared with monocytes. In this system, the differentiated macrophages thus show stronger responses to CCL3 than monocytes in chemotaxis and intracellular calcium flux assays, whereas responses to CCL2 are the opposite. The differential responsiveness of monocytes and macrophages to distinct sets of chemokines can explain why an impaired CCL3–CCR1 axis reduces retention of MAMs without affecting initial recruitment of IMs (Fig. 7 A).

Our results indicate that activation of the CCL3–CCR1 axis prolongs retention of MAMs in the lung at least in part through integrin α4. We also show that activation of the CCL3–CCR1 axis enhances adhesion of macrophages to VCAM-1 expressing cancer cells via integrin α4. In myeloma cells, CCL3 can increase the expression of integrin β1, which forms a heterodimer with integrin α4 and binds to the ligands such as fibronectin and VCAM-1 (Oba et al., 2005). In our metastasis model, however, the MAMs isolated from WT and *Ccr1*$^{-/-}$ mice expressed comparable levels of integrin α4 and β1 mRNA and protein (unpublished data), suggesting that the CCL3–CCR1 axis might regulate adhesive configurations of integrins rather than their expression. Similar results are reported in the in vitro T cell adhesion assay (Lloyd et al., 1996). Namely, CCL3 induces T cell adhesion to recombinant VCAM-1 that is suppressed by anti-integrin α4 neutralizing antibody, whereas CCL3 does not alter surface expression of integrins. CCL3 can also increase adhesion of hematopoietic progenitor cells to fibronectin (Suehiro et al., 1999). The effect of CCL3 on the progenitor cells is inhibited by blocking antibodies against integrins α4 and β1, although CCL3 does not alter integrin expression. Interestingly, when these progenitor cells are exposed to CCL3, the amount of F-actin in the cell cortex is increased within 60 s. Although the precise mechanism remains undefined, it is possible that the CCL3–CCR1 axis regulates conformational changes and/or clustering of integrins through the polymerization of cytoskeletal actin that is associated with the endodomain of integrins.

Breast cancer cells frequently metastasize to the bone and lung, which makes breast cancer a leading cause of cancer death. Unfortunately, current therapies are not sufficient to prevent it probably because of resistance by rapid evolution of mutation-prone cancer cells. A newly appreciated target for therapy is the tumor microenvironment (Joyce and Pollard, 2009;

Hanahan and Coussens, 2012) and particularly macrophages within it because they promote breast cancer metastasis (Qian and Pollard, 2010) and they are not prone to hypermutation. CCL2 is one target fitting this strategy as it recruits MAMs that promote metastasis (Qian et al., 2011). Indeed, anti-CCL2 antibodies suppress distant metastases and improve overall survival in preclinical models (Lu and Kang, 2009; Qian et al., 2011; Zhu et al., 2011). However, humanized anti-CCL2 antibody is ineffective at achieving biological effects in humans due to a feedback mechanism that increases CCL2 production (Sandu et al., 2013), which suggests difficulty in suppressing the IM recruitment by CCL2 deprivation. Furthermore, loss of CCL2 signaling in mouse models severely depresses the numbers of circulating monocytes and increases susceptibility to infection (Serbina et al., 2008). A recent paper also suggests a risk of anti-CCL2 therapy as there is a rebound increase of prometastatic myeloid cells after cessation of the therapy that accelerates the metastatic diseases (Bonapace et al., 2014). Here, we show that human and mouse macrophages secrete CCL3 through activation of CCL2 signaling. Deletion of CCL3 or its receptor CCR1 in macrophages reduces the number of lung metastasis foci developed by human and mouse breast cancer cells, as well as the number of MAMs accumulated in tumor-challenged lung without inhibiting circulating monocyte number. Because the suppressive effect of *Ccl3* gene ablation is comparable with *Ccr2* knockout and antibody treatment inhibits metastasis (Fig. 4, A and B), these results suggest that inhibition of the CCL2-induced chemokine cascade is effective in preventing breast cancer metastasis and suggests that CCR1 antagonists as a better therapeutic option. Supporting this proposal, recent clinical trials in rheumatoid arthritis indicate that CCR1 antagonists show clinical activity without feedback-related increases in CCR1 ligands, suppressive effects on monocytes, or adverse events including increased risk of infections (Dairaghi et al., 2011; Tak et al., 2013).

It has been reported that CCR1 can also regulate trafficking of potentially tumoricidal immune cells such as T cells (Schaller et al., 2008), NK cells (Bernardini et al., 2008), and dendritic cells (Iida et al., 2008). Although an impact of CCR1 activation in these cells on tumor metastasis is largely unknown, it seems to play a minor role in some types of tumors because prolonged treatment with CCR1 antagonists suppresses multiple myeloma tumor burden in the bone (Dairaghi et al., 2012) and colon cancer liver metastasis (Kitamura et al., 2010). These studies, as well as our current results, suggest the therapeutic potential of CCR1 antagonists in metastatic progression of certain tumor types, including breast cancer.

MATERIALS AND METHODS

Cell lines, primary samples, and cell culture. We obtained E0771 mouse mammary adenocarcinoma cells derived from a medullary cancer (Ewens et al., 2005) from E. Mihich (Rosewell Park Cancer Institute, Buffalo, NY). To obtain highly metastatic populations, we injected E0771 cells i.v. into C57BL/6 mice, and cultured the cells isolated from lung metastatic foci (E0771-LG). Human breast cancer cells MDA-MB-435, MDA-MB-231, T47D, and MCF7 were provided by P. Kenny and O. Giricz (Albert Einstein College of Medicine, Bronx, NY), and MDA-MB-231:4175TGL clone was provided by J. Massagué (Memorial Sloan-Kettering Cancer Center, New York, NY). All cancer cells were cultured in DMEM supplemented with 10% (vol/vol) FBS. Mouse BM derived macrophages (BMDMs) were isolated as described previously (Tushinski et al., 1982) and cultured in αMEM supplemented with 10% FBS and 10^4 U/ml human recombinant CSF-1. In some experiments, the BMDMs are cultured with recombinant mouse CCL2 (PeproTech; endotoxin level is <0.1 ng/μg of protein) for 12 h. Human blood (buffy coats) was obtained from New York Blood Services under informed consent, which is approved by Albert Einstein College of Medicine Institutional Review Board. Peripheral blood mononuclear cells (PBMCs) were isolated as described previously (Cassetta et al., 2013), and monocytes were isolated using the Macs Monocyte isolation kit II (Miltenyi Biotec). The isolated monocytes were cultured in αMEM supplemented with 10% FBS and 10^4 U/ml CSF-1 for 7 d to differentiate them into macrophages. In some experiments, the human macrophages were cultured in αMEM supplemented with 10% FBS and 10^3 U/ml human recombinant CSF-1 or the same medium that had been conditioned from human breast cancer cells for 24 h.

Mice. *Ccr2*$^{-/-}$, *Ccl3*$^{-/-}$, *Ccr5*$^{-/-}$, ROSA-rtTA, and *tetO-Cre* mice on the C57BL/6 genetic background were purchased from The Jackson Laboratory. *Ccr1*$^{-/-}$ (C57BL/6) and *Rag2*$^{-/-}$ mice were purchased from Taconic. We obtained transgenic mice expressing PyMT oncogene under the control of MMTV-LTR promoter (PyMT) on the FVB background from W.J. Muller (McGill University, Montreal, Canada) and those backcrossed with C57BL/6 mice (PyMT BL6) from S.J. Gendler (Mayo Clinic, Phoenix, AZ). The PyMT BL6 or *Rag2*$^{-/-}$ mice were further crossed with *Ccl3*$^{-/-}$ mice to construct PyMT:*Ccl3*$^{-/-}$ or *Rag2*$^{-/-}$:*Ccl3*$^{-/-}$ compound mutants. We have constructed a conditional knockout strain for CSF-1 receptor that is essential for survival of distinct populations of myeloid cells (Li et al., 2006). The B6.Cg-*Csf1r*^{tm1Jwp}/J (*Csf1r*$^{F/F}$) mice were crossed with ROSA-rtTA and tetO-Cre mice to construct rtTA:tetO-Cre:*Csf1r*$^{F/F}$ mice, in which inflammatory monocytes are depleted by loss of *Csf1r* after doxycycline treatment. 7–8-wk-old female mice were used unless described specifically. All animals were randomly allocated by genotype. All procedures involving mice were conducted in accordance with National Institutes of Health regulations concerning the care and use of experimental animals. Experimental procedures were approved by Institutional Animal Care & Use Committee of the Albert Einstein College of Medicine.

BMT. BM cells were isolated from C57BL/6, *Ccl3*$^{-/-}$, *Ccr1*$^{-/-}$, *Rag2*$^{-/-}$, or *Rag2*$^{-/-}$*Ccl3*$^{-/-}$ mice. BM cells were counted in a hemocytometer and resuspended at 2×10^7 cells/ml in PBS. The 4-wk-old recipient mice (C57BL/6 or *nu/nu* mice) were irradiated with 9 Gy γ-rays and transplanted with 4×10^6 donor cells i.v.. The recipient mice were used for experiments 6–8 wk later.

Experimental metastasis assay. 4×10^5 E0771-LG cells were injected into the tail vein of C57BL/6 or knockout mice (7-wk-old female). In cases where the mice had received BMT, the number of cells injected was reduced to 3×10^5. To deplete CSF-1–dependent myeloid cells, we gave doxycycline in the drinking water to the rtTA:tetO-Cre:*Csf1r*$^{F/F}$ mice from 7 d before tumor injection to the endpoint. We also injected 10^6 Met-1 cells into the tail vein of FVB females. We euthanized the mice 11 d (E0771-LG) or 14 d (Met-1) after tumor cell injection, and dissected the lung to prepare H&E sections as described previously (Qian et al., 2011). Lung images of all five lobes were taken using a Zeiss SV11 microscope with a Retiga 1300 digital camera via 2× objective lens, and analyzed using Fiji software to determine the average number of metastasis nodules per mm^2 of lung area. The average size of nodules (total nodule area [mm^2]/total nodule number) is also determined and converted to the average diameter (mm). 10^6 MDA-MB-231:4175 human breast cancer cells were injected into the mammary fat pad of *nu/nu* mice that received BM cells from *Rag2*$^{-/-}$ or *Rag2*$^{-/-}$*Ccl3*$^{-/-}$ mice. After 4 wk, we dissected the primary tumor and determined tumor loads in the lung area by in vivo bioluminescence imaging every week.

Antibody treatment. The mice injected with 4×10^5 E0771-LG cells received anti–mouse CCL2 neutralizing antibody or control isotype matched IgG (5 mg/kg body weight) via i.p. injection on days 9 and 10 after tumor injection. 24 h after the last treatment, the mice were euthanized to isolate monocytes and macrophages. To neutralize CCL3, the FVB mice injected 10^6 Met-1 cells received anti–mouse CCL3 antibody or control IgG (R&D Systems; 5 mg/kg body weight) via i.p. injection 2 h before and 24 h after tumor injection. To deplete neutrophils, anti–mouse Ly6G neutralizing antibodies or control isotype matched IgG (BioLegend) were given at 1 mg/kg body weight via i.p. injection before 24 and 5 h, and after 16 h of tumor injection.

In vivo bioluminescence imaging. We injected 100 µl of D-luciferin solution (10 mg/ml in PBS, i.v.; GoldBio) into anesthetized tumor-bearing mice. Bioluminescence from the luciferase-expressing tumor cells was determined using IVIS-SPECTRUM in vivo photon-counting device (Caliper Life Sciences). Images were quantified as photon counts/second using the Living Image software (Caliper Life Sciences).

Adoptive transfer of monocytes. In metastasis assay, $CD11b^+Ly6C^+Ly6G^-$ cells were sorted from BM monocytes isolated from WT or *Ccl3*$^{-/-}$ mice and enriched by Monocyte Isolation kit (Miltenyi Biotec). Sorted cells (10^6) were injected with 5×10^5 of E0771-LG cells into mice transplanted with *Ccl3*$^{-/-}$ BM cells. To chase the cell fate, monocytes were sorted from C57BL/6 or *Ccr1*$^{-/-}$ mice and labeled with CellTracker CMFDA (Invitrogen) following the manufacturer's instructions. The labeled monocytes (5×10^5) were transferred into C57BL/6 mice bearing pulmonary metastases. Pulmonary tumor burdens in the recipients were determined by in vivo bioluminescence imaging one day before monocyte transfer. The tumor-bearing mice were allocated to each group equally by their tumor loads. Some recipient mice were treated with anti-integrin α4 antibodies (5 mg/kg body weight, i.p.; BioLegend) 18 h after transfer.

Flow cytometry and sorting. Single-cell suspensions were prepared from perfused lungs or blood samples as described previously (Qian et al., 2011). After blocking with anti–mouse CD16/CD32 antibody (BD), the cells were stained with DAPI and fluorescent antibodies to following antigens; CD45 (30-F11), F4/80 (BM8), CD11b (M1/70), Ly6C (HK1.4), Gr1 (RB6-8C5), CD115 (AFS98), CD3 (17A2), NK1.1 (PK136; all from BioLegend); CD4 (GK1.5), B2.20 (RA3-6B2), Ly6G (1A8), CD11c (HL3; all from BD); CD8a (53–6.7), CCR5 (7A4; both from eBioscience); CCR1 (643854), CCR2 (475301; both from R&D Systems). Flow cytometry was performed using LSRII cytometer (BD) and analyzed using FlowJo software (Tree Star). In some experiments, the stained cells were sorted using FACSAria II (BD).

Microarray analysis. We isolated MAMs ($F4/80^+$ $CD11b^+$) from the tumor-bearing lung by FACS Aria (BD) using above-mentioned antibodies. We also collected pulmonary resident macrophages ($F4/80^+$ $CD11c^+$) and splenic macrophages ($F4/80^+$ $CD11b^+$) from healthy mice. We extracted RNA from these cells and used it for hybridization on Nimblegen Mouse Gene Expression Array Chips. We performed ANOVA test to identify genes that are significantly ($P < 0.01$) changed in MAMs (more than threefold change) compared with resident macrophages. All gene expression datasets used in this study are available at the Gene Expression Omnibus accession no. GSE68862.

PCR. Expression of mRNA was determined by RT-PCR using SuperScript III (Invitrogen) and ExTaq (Takara). All real-time PCR was performed on Opticon 2 qPCR (MJ Research) using SYBR master mix (Invitrogen). Primers used for real-time PCR are: mouse *Gapdh*, 5′-AGAACATCATCCCTGCATCC-3′ and 5′-CACATTGGGGGTAGGAACAC-3′; mouse *Cd3*, 5′-ACCATGACACTCTGCAACCA-3′ and 5′-GATGAATTGGCGTGGAATCT-3′; mouse *Ccr1*, 5′-ACTCCACTCCATGCCAAAAG-3′ and 5′-CTAGGACATTGCCCACCACT-3′; mouse *Ccr5*, 5′-CGAAAACACATGGTCAAACG-3′ and 5′-GTTCTCCTGTGGATCGGGTA-3′; human *GAPDH*, 5′-CAGCCTCAAGATCATCAGCA-3′ and 5′-TGTGGTCATGAGTCCTTCCA-3′; human *CCL3*, 5′-TGCAACCAGTTCTCTGCATC-3′ and 5′-TGGCTGCTCGTCTCAAAGTA-3′. Primers used for RT-PCR are: mouse *Gapdh*, 5′-ACTCCACTCACGGCAAATTC-3′ and 5′-CCTTCCACAATGCCAAAGTT-3′ (370 bp); mouse *Ccl2*, 5′-CCCAATGAGTAGGCTGGAGA-3′ and 5′-AAAATGGATCCACACCTTGC-3′ (434 bp); mouse *Ccl3*, 5′-ATGAAGGTCTCCACCACTGC-3′ and 5′-CCCAGGTCTCTTTGGAGTCA-3′ (279 bp); mouse *Ccr1*, 5′-ACTCCACTCCATGCCAAAAG-3′ and 5′-GCAAACACAGCATGGACAAT-3′ (364 bp); mouse *Ccr2*, 5′-GGGCTCACTATGCTGCAAAT-3′ and 5′-CGAAACAGGGTGTGGAGAAT-3′ (400 bp); mouse *Ccr5*, 5′-ATTCTCCACACCCTGTTTCG-3′ and 5′-GTTCTCCTGTGGATCGGGTA-3′ (388 bp); human *GAPDH*, 5′-ACCCAGAAGACTGTGGATGG-3′ and 5′-CCCTGTTGCTGTAGCCAAAT-3′ (421 bp); human *CCL3*, 5′-ATGCAGGTCTCCACTGCTG-3′ (279 bp); human *CCR1*, 5′-GCAGCCTTCACTTTCCTCAC-3′ and 5′-AGAGGAAGGGGAGCCATTTA-3′ (447 bp); human *CCR5*, 5′-TAGTCATCTTGGGGCTGGTC-3′ and 5′-TGAACTTCTCCCCGACAAAG-3′ (321 bp).

ELISA. Mouse BM macrophages or human breast cancer cells were cultured in αMEM supplemented with 10% (vol/vol) FBS and 10^3 U/ml human recombinant CSF-1 for 12 or 24 h, respectively. Conditioned media were collected from the cultured cells, and the levels of mouse CCL3 (MIP-1α) or human CCL2 (MCP-1) were determined using the Mouse MIP-1 α ELISA kit or Human CCL2 (MCP-1) ELISA kit (eBioscience), respectively. Samples were collected independently and analyzed by one assay.

In vitro extravasation assay. The extravasation assay was performed as described previously (Qian et al., 2011). In brief, 2×10^4 3B-11 mouse endothelial cells (American Type Culture Collection) were cultured on top of GFR Matrigel invasion chambers (BD Biosciences) for 2 d to make a monolayer. BMDMs (2×10^4) were loaded to the bottom of the chambers put into a plate-well with DMEM including 10%FBS and 10^4 U/ml CSF-1 to allow attachment. E0771-LG or Met-1 cells (2×10^4) labeled with CellTracker CMFDA were loaded into the insert with DMEM including 0.5% FBS and 10^4 U/ml CSF-1. After 36 h, the chambers were fixed with 4% paraformaldehyde, and cells on top were removed. Fluorescent images of 5 randomly selected fields in each insert were captured with Olympus IX81 fluorescence microscope and numbers of cancer cells migrated through endothelial monolayer were counted using Fiji software.

In vitro interaction assay. BMDMs and E0771-LG cells were labeled with CellTracker CMTMR and CMFDA (Invitrogen), respectively. To determine dynamic interaction between BMDMs and cancer cells, single cell suspension of each cells (10^4) were placed on Matrigel (5 mg/ml) and cultured for 1 h in αMEM supplemented with 10%FBS and 10^4U/ml CSF-1. Bright-field and fluorescent images (10 randomly selected fields in each well) were acquired every 10 min by fluorescence microscopy (Axiovert 200). Movies of BMDMs were tracked in Fiji ImageJ and tracks were analyzed in Mathematica (Wolfram) to determine the duration of interaction between BMDMs and cancer cells. To detect BMM binding to cancer cells, single cell suspension of each labeled cells (5×10^5) were mixed in v-bottom 96-well plates and cultured for 1 h in αMEM supplemented with 10%FBS and 10^4 U/ml CSF-1. The ratio of CMFTMR/CMFDA double-positive population was determined by flow cytometry. Based on a side-scattered light (SSC), we confirmed that >80% of double-positive fraction consists doublet of cells whereas <10% of single positive fraction does. To maintain binding activity of integrin, the cells were kept in Hepes buffer containing $CaCl_2$ and $MgCl_2$ during the analysis.

Immunofluorescence staining. E0771-LG cells (10^6) labeled with CellTracker CMFDA (Invitrogen) were injected into the mice. After 20 h, the lungs were dissected and directly embedded in O.C.T. compound (Sakura Finetek). Sections were fixed with cold acetone, immunostained with rat monoclonal antibodies to CD11b (1:100; BD) followed by Alexa Fluor 546

anti–rat IgG (1:250; Molecular Probes), and mounted with VECTASHIELD with DAPI (Vector Laboratories). Fluorescent images were captured and analyzed with Olympus IX81 fluorescence microscope and Adobe Photoshop software.

Statistical analysis. Sample size was determined based on a relative standard deviation from our previous studies. All samples were collected independently and analyzed by at least two independent experiments. Data were analyzed by Student's *t* test and are expressed as mean ± SEM. P-values <0.05 were considered significant.

Online supplemental material. Fig. S1 shows the FACS gating strategy to identify myeloid cell populations quantified in Figs. 2, 5, and 6. Video 1 and Video 2 show time lapse imaging of interactions between WT (S1) or *Ccr1*$^{-/-}$ (S2) BMDMs and E0771 cancer cells. Online supplemental material is available at http://www.jem.org/cgi/content/full/jem.20141836/DC1.

We thank R. Stanley and V. Chitu for technical advice about macrophage culture, E. Mihich for providing E0771 cells, J. Massagué for providing MDA-MB-231:4175TGL clone, P. Kenny and O. Giricz for providing human breast cancer cells, S.J. Gendler for providing PyMT BL6 mice, and J. Zhang and G. Simkin for technical support for FACS.

This work was supported by United States Department of Defense Congressionally Directed Medical Research Programs (DOD#W81xWH-11-1-0703), National Institutes of Health grants RO1 CA172451 and PO1 CA100324 and the Wellcome Trust 101067/Z/13/Z, UK.

J.W. Pollard has patent applications pending for macrophages synthesized molecules in the treatment of metastasis. The authors declare no additional competing financial interests.

Author contributions: T. Kitamura and J.W. Pollard designed the research and analyzed data. T. Kitamura performed and analyzed the in vitro and in vivo data. B-Z. Qian generated the microarray data. D. Soong established and performed the in vitro interaction assay. R. Noy and J. Li generated the PyMT:Ccl3$^{-/-}$ mice. L. Cassetta provided human monocytes. G. Sugano developed the analytic program. Y. Kato established the in vitro interaction assay. T. Kitamura and J.W. Pollard wrote the manuscript.

Submitted: 22 September 2014
Accepted: 11 May 2015

REFERENCES

Bernardini, G., G. Sciumè, D. Bosisio, S. Morrone, S. Sozzani, and A. Santoni. 2008. CCL3 and CXCL12 regulate trafficking of mouse bone marrow NK cell subsets. *Blood*. 111:3626–3634. http://dx.doi.org/10.1182/blood-2007-08-106203

Bingle, L., N.J. Brown, and C.E. Lewis. 2002. The role of tumour-associated macrophages in tumour progression: implications for new anticancer therapies. *J. Pathol.* 196:254–265. http://dx.doi.org/10.1002/path.1027

Bonapace, L., M.M. Coissieux, J. Wyckoff, K.D. Mertz, Z. Varga, T. Junt, and M. Bentires-Alj. 2014. Cessation of CCL2 inhibition accelerates breast cancer metastasis by promoting angiogenesis. *Nature*. 515:130–133. http://dx.doi.org/10.1038/nature13862

Borowsky, A.D., R. Namba, L.J.T. Young, K.W. Hunter, J.G. Hodgson, C.G. Tepper, E.T. McGoldrick, W.J. Muller, R.D. Cardiff, and J.P. Gregg. 2005. Syngeneic mouse mammary carcinoma cell lines: two closely related cell lines with divergent metastatic behavior. *Clin. Exp. Metastasis*. 22:47–59. http://dx.doi.org/10.1007/s10585-005-2908-5

Cain, D.W., P.B. Snowden, G.D. Sempowski, and G. Kelsoe. 2011. Inflammation triggers emergency granulopoiesis through a density-dependent feedback mechanism. *PLoS ONE*. 6:e19957. http://dx.doi.org/10.1371/journal.pone.0019957

Cassetta, L., A. Kajaste-Rudnitski, T. Coradin, E. Saba, G. Della Chiara, M. Barbagallo, F. Graziano, M. Alfano, E. Cassol, E. Vicenzi, and G. Poli. 2013. M1 polarization of human monocyte-derived macrophages restricts pre and postintegration steps of HIV-1 replication. *AIDS*. 27:1847–1856. http://dx.doi.org/10.1097/QAD.0b013e328361d059

Chen, Q., X.H. Zhang, and J. Massagué. 2011. Macrophage binding to receptor VCAM-1 transmits survival signals in breast cancer cells that invade the lungs. *Cancer Cell*. 20:538–549. http://dx.doi.org/10.1016/j.ccr.2011.08.025

Dairaghi, D.J., P. Zhang, Y. Wang, L.C. Seitz, D.A. Johnson, S. Miao, L.S. Ertl, Y. Zeng, J.P. Powers, A.M. Pennell, et al. 2011. Pharmacokinetic and pharmacodynamic evaluation of the novel CCR1 antagonist CCX354 in healthy human subjects: implications for selection of clinical dose. *Clin. Pharmacol. Ther.* 89:726–734. http://dx.doi.org/10.1038/clpt.2011.33

Dairaghi, D.J., B.O. Oyajobi, A. Gupta, B. McCluskey, S. Miao, J.P. Powers, L.C. Seitz, Y. Wang, Y. Zeng, P. Zhang, et al. 2012. CCR1 blockade reduces tumor burden and osteolysis in vivo in a mouse model of myeloma bone disease. *Blood*. 120:1449–1457. http://dx.doi.org/10.1182/blood-2011-10-384784

Davies, L.C., S.J. Jenkins, J.E. Allen, and P.R. Taylor. 2013. Tissue-resident macrophages. *Nat. Immunol.* 14:986–995. http://dx.doi.org/10.1038/ni.2705

Eis, V., B. Luckow, V. Vielhauer, J.T. Siveke, Y. Linde, S. Segerer, G. Perez De Lema, C.D. Cohen, M. Kretzler, M. Mack, et al. 2004. Chemokine receptor CCR1 but not CCR5 mediates leukocyte recruitment and subsequent renal fibrosis after unilateral ureteral obstruction. *J. Am. Soc. Nephrol.* 15:337–347. http://dx.doi.org/10.1097/01.ASN.0000111246.87175.32

Ewens, A., E. Mihich, and M.J. Ehrke. 2005. Distant metastasis from subcutaneously grown E0771 medullary breast adenocarcinoma. *Anticancer Res.* 25(6B):3905–3915.

Farmer, P., H. Bonnefoi, V. Becette, M. Tubiana-Hulin, P. Fumoleau, D. Larsimont, G. Macgrogan, J. Bergh, D. Cameron, D. Goldstein, et al. 2005. Identification of molecular apocrine breast tumours by microarray analysis. *Oncogene*. 24:4660–4671. http://dx.doi.org/10.1038/sj.onc.1208561

Finak, G., N. Bertos, F. Pepin, S. Sadekova, M. Souleimanova, H. Zhao, H. Chen, G. Omeroglu, S. Meterissian, A. Omeroglu, et al. 2008. Stromal gene expression predicts clinical outcome in breast cancer. *Nat. Med.* 14:518–527. http://dx.doi.org/10.1038/nm1764

Fischer, F.R., Y. Luo, M. Luo, L. Santambrogio, and M.E. Dorf. 2001. RANTES-induced chemokine cascade in dendritic cells. *J. Immunol.* 167:1637–1643. http://dx.doi.org/10.4049/jimmunol.167.3.1637

Franklin, R.A., W. Liao, A. Sarkar, M.V. Kim, M.R. Bivona, K. Liu, E.G. Pamer, and M.O. Li. 2014. The cellular and molecular origin of tumor-associated macrophages. *Science*. 344:921–925. http://dx.doi.org/10.1126/science.1252510

Hanahan, D., and L.M. Coussens. 2012. Accessories to the crime: functions of cells recruited to the tumor microenvironment. *Cancer Cell*. 21:309–322. http://dx.doi.org/10.1016/j.ccr.2012.02.022

Huffnagle, G.B., R.M. Strieter, L.K. McNeil, R.A. McDonald, M.D. Burdick, S.L. Kunkel, and G.B. Toews. 1997. Macrophage inflammatory protein-1α (MIP-1α) is required for the efferent phase of pulmonary cell-mediated immunity to a Cryptococcus neoformans infection. *J. Immunol.* 159:318–327.

Hussell, T., and T.J. Bell. 2014. Alveolar macrophages: plasticity in a tissue-specific context. *Nat. Rev. Immunol.* 14:81–93. http://dx.doi.org/10.1038/nri3600

Iida, N., Y. Nakamoto, T. Baba, K. Kakinoki, Y.Y. Li, Y. Wu, K. Matsushima, S. Kaneko, and N. Mukaida. 2008. Tumor cell apoptosis induces tumor-specific immunity in a CC chemokine receptor 1- and 5-dependent manner in mice. *J. Leukoc. Biol.* 84:1001–1010. http://dx.doi.org/10.1189/jlb.1107791

Jemal, A., F. Bray, M.M. Center, J. Ferlay, E. Ward, and D. Forman. 2011. Global cancer statistics. *CA Cancer J. Clin.* 61:69–90. http://dx.doi.org/10.3322/caac.20107

Joyce, J.A., and J.W. Pollard. 2009. Microenvironmental regulation of metastasis. *Nat. Rev. Cancer.* 9:239–252. http://dx.doi.org/10.1038/nrc2618

Kaufmann, A., R. Salentin, D. Gemsa, and H. Sprenger. 2001. Increase of CCR1 and CCR5 expression and enhanced functional response to

MIP-1 α during differentiation of human monocytes to macrophages. *J. Leukoc. Biol.* 69:248–252.

Kitamura, T., T. Fujishita, P. Loetscher, L. Revesz, H. Hashida, S. Kizaka-Kondoh, M. Aoki, and M.M. Taketo. 2010. Inactivation of chemokine (C-C motif) receptor 1 (CCR1) suppresses colon cancer liver metastasis by blocking accumulation of immature myeloid cells in a mouse model. *Proc. Natl. Acad. Sci. USA.* 107:13063–13068. http://dx.doi.org/10.1073/pnas.1002372107

Knowles, H.J., and A.L. Harris. 2007. Macrophages and the hypoxic tumour microenvironment. *Front. Biosci.* 12:4298–4314. http://dx.doi.org/10.2741/2389

Leek, R.D., C.E. Lewis, R. Whitehouse, M. Greenall, J. Clarke, and A.L. Harris. 1996. Association of macrophage infiltration with angiogenesis and prognosis in invasive breast carcinoma. *Cancer Res.* 56:4625–4629.

Li, J., K. Chen, L. Zhu, and J.W. Pollard. 2006. Conditional deletion of the colony stimulating factor-1 receptor (c-fms proto-oncogene) in mice. *Genesis.* 44:328–335. http://dx.doi.org/10.1002/dvg.20219

Lin, E.Y., A.V. Nguyen, R.G. Russell, and J.W. Pollard. 2001. Colony-stimulating factor 1 promotes progression of mammary tumors to malignancy. *J. Exp. Med.* 193:727–740. http://dx.doi.org/10.1084/jem.193.6.727

Lin, E.Y., J.G. Jones, P. Li, L. Zhu, K.D. Whitney, W.J. Muller, and J.W. Pollard. 2003. Progression to malignancy in the polyoma middle T oncoprotein mouse breast cancer model provides a reliable model for human diseases. *Am. J. Pathol.* 163:2113–2126. http://dx.doi.org/10.1016/S0002-9440(10)63568-7

Lloyd, A.R., J.J. Oppenheim, D.J. Kelvin, and D.D. Taub. 1996. Chemokines regulate T cell adherence to recombinant adhesion molecules and extracellular matrix proteins. *J. Immunol.* 156:932–938.

Lu, X., and Y. Kang. 2009. Chemokine (C-C motif) ligand 2 engages $CCR2^+$ stromal cells of monocytic origin to promote breast cancer metastasis to lung and bone. *J. Biol. Chem.* 284:29087–29096. http://dx.doi.org/10.1074/jbc.M109.035899

Luo, Y., F.R. Fischer, W.W. Hancock, and M.E. Dorf. 2000. Macrophage inflammatory protein-2 and KC induce chemokine production by mouse astrocytes. *J. Immunol.* 165:4015–4023. http://dx.doi.org/10.4049/jimmunol.165.7.4015

Matsushima, K., C.G. Larsen, G.C. DuBois, and J.J. Oppenheim. 1989. Purification and characterization of a novel monocyte chemotactic and activating factor produced by a human myelomonocytic cell line. *J. Exp. Med.* 169:1485–1490. http://dx.doi.org/10.1084/jem.169.4.1485

Minn, A.J., G.P. Gupta, P.M. Siegel, P.D. Bos, W. Shu, D.D. Giri, A. Viale, A.B. Olshen, W.L. Gerald, and J. Massagué. 2005. Genes that mediate breast cancer metastasis to lung. *Nature.* 436:518–524. http://dx.doi.org/10.1038/nature03799

Nakasone, Y., M. Fujimoto, T. Matsushita, Y. Hamaguchi, D.L. Huu, M. Yanaba, S. Sato, K. Takehara, and M. Hasegawa. 2012. Host-derived MCP-1 and MIP-1α regulate protective anti-tumor immunity to localized and metastatic B16 melanoma. *Am. J. Pathol.* 180:365–374. http://dx.doi.org/10.1016/j.ajpath.2011.09.005

Neote, K., D. DiGregorio, J.Y. Mak, R. Horuk, and T.J. Schall. 1993. Molecular cloning, functional expression, and signaling characteristics of a C-C chemokine receptor. *Cell.* 72:415–425. http://dx.doi.org/10.1016/0092-8674(93)90118-A

Oba, Y., J.W. Lee, L.A. Ehrlich, H.Y. Chung, D.F. Jelinek, N.S. Callander, R. Horuk, S.J. Choi, and G.D. Roodman. 2005. MIP-1α utilizes both CCR1 and CCR5 to induce osteoclast formation and increase adhesion of myeloma cells to marrow stromal cells. *Exp. Hematol.* 33:272–278. http://dx.doi.org/10.1016/j.exphem.2004.11.015

Ojalvo, L.S., W. King, D. Cox, and J.W. Pollard. 2009. High-density gene expression analysis of tumor-associated macrophages from mouse mammary tumors. *Am. J. Pathol.* 174:1048–1064. http://dx.doi.org/10.2353/ajpath.2009.080676

Pollard, J.W. 2009. Trophic macrophages in development and disease. *Nat. Rev. Immunol.* 9:259–270. http://dx.doi.org/10.1038/nri2528

Prest, S.J., R.C. Rees, C. Murdoch, J.F. Marshall, P.A. Cooper, M. Bibby, G. Li, and S.A. Ali. 1999. Chemokines induce the cellular migration of MCF-7 human breast carcinoma cells: subpopulations of tumour cells display positive and negative chemotaxis and differential in vivo growth potentials. *Clin. Exp. Metastasis.* 17:389–396. http://dx.doi.org/10.1023/A:1006657109866

Qian, B.-Z., and J.W. Pollard. 2010. Macrophage diversity enhances tumor progression and metastasis. *Cell.* 141:39–51. http://dx.doi.org/10.1016/j.cell.2010.03.014

Qian, B., Y. Deng, J.H. Im, R.J. Muschel, Y. Zou, J. Li, R.A. Lang, and J.W. Pollard. 2009. A distinct macrophage population mediates metastatic breast cancer cell extravasation, establishment and growth. *PLoS ONE.* 4:e6562. http://dx.doi.org/10.1371/journal.pone.0006562

Qian, B.-Z., J. Li, H. Zhang, T. Kitamura, J. Zhang, L.R. Campion, E.A. Kaiser, L.A. Snyder, and J.W. Pollard. 2011. CCL2 recruits inflammatory monocytes to facilitate breast-tumour metastasis. *Nature.* 475:222–225. http://dx.doi.org/10.1038/nature10138

Ramos, C.D.L., C. Canetti, J.T. Souto, J.S. Silva, C.M. Hogaboam, S.H. Ferreira, and F.Q. Cunha. 2005. MIP-1α[CCL3] acting on the CCR1 receptor mediates neutrophil migration in immune inflammation via sequential release of TNF-α and LTB4. *J. Leukoc. Biol.* 78:167–177. http://dx.doi.org/10.1189/jlb.0404237

Roca, H., Z.S. Varsos, S. Sud, M.J. Craig, C. Ying, and K.J. Pienta. 2009. CCL2 and interleukin-6 promote survival of human $CD11b^+$ peripheral blood mononuclear cells and induce M2-type macrophage polarization. *J. Biol. Chem.* 284:34342–34354. http://dx.doi.org/10.1074/jbc.M109.042671

Rodero, M.P., C. Auvynet, L. Poupel, B. Combadière, and C. Combadière. 2013. Control of both myeloid cell infiltration and angiogenesis by CCR1 promotes liver cancer metastasis development in mice. *Neoplasia.* 15:641–648. http://dx.doi.org/10.1593/neo.121866

Sandhu, S.K., K. Papadopoulos, P.C. Fong, A. Patnaik, C. Messiou, D. Olmos, G. Wang, B.J. Tromp, T.A. Puchalski, F. Balkwill, et al. 2013. A first-in-human, first-in-class, phase I study of carlumab (CNTO 888), a human monoclonal antibody against CC-chemokine ligand 2 in patients with solid tumors. *Cancer Chemother. Pharmacol.* 71:1041–1050. http://dx.doi.org/10.1007/s00280-013-2099-8

Schall, T.J., and A.E.I. Proudfoot. 2011. Overcoming hurdles in developing successful drugs targeting chemokine receptors. *Nat. Rev. Immunol.* 11:355–363. http://dx.doi.org/10.1038/nri2972

Schaller, M.A., L.E. Kallal, and N.W. Lukacs. 2008. A key role for CC chemokine receptor 1 in T-cell-mediated respiratory inflammation. *Am. J. Pathol.* 172:386–394. http://dx.doi.org/10.2353/ajpath.2008.070537

Serbina, N.V., T. Jia, T.M. Hohl, and E.G. Pamer. 2008. Monocyte-mediated defense against microbial pathogens. *Annu. Rev. Immunol.* 26:421–452. http://dx.doi.org/10.1146/annurev.immunol.26.021607.090326

Suehiro, Y., K. Muta, T. Umemura, Y. Abe, J. Nishimura, and H. Nawata. 1999. Macrophage inflammatory protein 1α enhances in a different manner adhesion of hematopoietic progenitor cells from bone marrow, cord blood, and mobilized peripheral blood. *Exp. Hematol.* 27:1637–1645. http://dx.doi.org/10.1016/S0301-472X(99)00103-4

Tak, P.P., A. Balanescu, V. Tseluyko, S. Bojin, E. Drescher, D. Dairaghi, S. Miao, V. Marchesin, J. Jaen, T.J. Schall, and P. Bekker. 2013. Chemokine receptor CCR1 antagonist CCX354-C treatment for rheumatoid arthritis: CARAT-2, a randomised, placebo controlled clinical trial. *Ann. Rheum. Dis.* 72:337–344. http://dx.doi.org/10.1136/annrheumdis-2011-201605

Tanaka, T., M. Terada, K. Ariyoshi, and K. Morimoto. 2010. Monocyte chemoattractant protein-1/CC chemokine ligand 2 enhances apoptotic cell removal by macrophages through Rac1 activation. *Biochem. Biophys. Res. Commun.* 399:677–682. http://dx.doi.org/10.1016/j.bbrc.2010.07.141

Tushinski, R.J., I.T. Oliver, L.J. Guilbert, P.W. Tynan, J.R. Warner, and E.R. Stanley. 1982. Survival of mononuclear phagocytes depends on a lineage-specific growth factor that the differentiated cells selectively destroy. *Cell.* 28:71–81. http://dx.doi.org/10.1016/0092-8674(82)90376-2

Wang, M.J., K.C.G. Jeng, and P.C. Shih. 2000. Differential expression and regulation of macrophage inflammatory protein (MIP)-1α and MIP-2 genes by alveolar and peritoneal macrophages in LPS-hyporesponsive C3H/HeJ mice. *Cell. Immunol.* 204:88–95. http://dx.doi.org/10.1006/cimm.2000.1697

Weber, C., K.S.C. Weber, C. Klier, S. Gu, R. Wank, R. Horuk, and P.J. Nelson. 2001. Specialized roles of the chemokine receptors CCR1 and

CCR5 in the recruitment of monocytes and T(H)1-like/CD45RO(+) T cells. *Blood*. 97:1144–1146. http://dx.doi.org/10.1182/blood.V97.4.1144

Wu, Y., Y.-Y. Li, K. Matsushima, T. Baba, and N. Mukaida. 2008. CCL3-CCR5 axis regulates intratumoral accumulation of leukocytes and fibroblasts and promotes angiogenesis in murine lung metastasis process. *J. Immunol.* 181:6384–6393. http://dx.doi.org/10.4049/jimmunol.181.9.6384

Youngs, S.J., S.A. Ali, D.D. Taub, and R.C. Rees. 1997. Chemokines induce migrational responses in human breast carcinoma cell lines. *Int. J. Cancer.* 71:257–266. http://dx.doi.org/10.1002/(SICI)1097-0215(19970410)71:2<257::AID-IJC22>3.0.CO;2-D

Zhu, X., M. Fujita, L.A. Snyder, and H. Okada. 2011. Systemic delivery of neutralizing antibody targeting CCL2 for glioma therapy. *J. Neurooncol.* 104:83–92. http://dx.doi.org/10.1007/s11060-010-0473-5